Journal Pre-proof

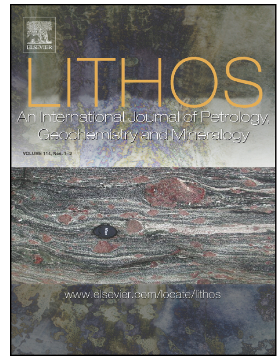

Plume-related Paranà-Etendeka igneous province: An evolution from plateau to continental rifting and breakup

L. Beccaluva, G. Bianchini, C. Natali, F. Siena

PII: S0024-4937(20)30121-3

DOI: https://doi.org/10.1016/j.lithos.2020.105484

Reference: LITHOS 105484

To appear in: *LITHOS*

Received date: 27 November 2019

Revised date: 10 March 2020

Accepted date: 11 March 2020

Please cite this article as: L. Beccaluva, G. Bianchini, C. Natali, et al., Plume-related Paranà-Etendeka igneous province: An evolution from plateau to continental rifting and breakup, *LITHOS* (2020), https://doi.org/10.1016/j.lithos.2020.105484

Plume-related Paranà-Etendeka igneous province: an evolution from plateau to continental rifting and breakup

Beccaluva L.[1], Bianchini G.[1], Natali C.[2],Siena F.[1]

[1]Department of Physics and Earth Sciences, University of Ferrara, Italy

[1]Department of Earth Sciences, University of Florence, Italy

Abstract

A critical review of the available multidisciplinary data on the Paranà-Etendeka Province allows for the reconciliation of the controversial aspects of its origin in a coherent tectonomagmatic scenario, in which continental flood basalt (CFB) magmatism evolved from the Paranà plateau *s.s.* (Stage 1) to progressive continental rifting in Etendeka (Stage 2), and then opened to the South Atlantic at the same latitude; the CFB magmatism is triggered by the prolonged impingement of the proto Tristan plume on the western Gondwana lithosphere. The provinciality of the CFB is evidenced by the incompatible element distribution and Sr-Nd-Pb isotopic data, where the Paranà and Etendeka magmas are more akin to lithospheric and asthenospheric (plume-related) components, respectively. **Stage 1** consisted of the rapid outpouring of the Paranà Plateau *s.s.* CFB (135–134 Ma, ~ 800 000 km^3, and eruption rate ~0.8 km^3/a) that was zonally arranged with prevailing high-TiO_2 (HT) basalts in the central-northern part and low-TiO_2 (LT) suites at the southern periphery. The differentiated nature (MgO=8–4 %) of these plateau magmas suggests the variable extent of fractional crystallisation during rise through a relatively thick lithosphere. Petrological modelling, isotopic signatures ($^{87}Sr/^{86}Sr$ 0.70483-0.70620, and $\varepsilon Nd_{(t)}$ from −1.27 to −5.78), and incompatible element distributions approaching the EM1 mantle component suggest that the HT and LT Paranà basalts may be derived from mantle sources located in the lower lithosphere at P 3–4 GPa and a potential temperature (T_p) of 1500–1550 °C. The high T_p recorded (and the relative T_{excess} 250–300 °C thermal anomaly) can be attained after several million years of lithospheric heating, beginning from the first plume impact, which is represented by precursor alkaline events (145–138 Ma) at the westernmost border of the Paranà plateau. The subsequent rifting (**Stage 2**, mostly 134–128 Ma) developed SE of the Paranà plateau in relation to the NW drifting of the Gondwana plate over the rising plume and was accompanied by progressive lithospheric arching, thinning, and rifting, which culminated in continental breakup close to the Etendeka border. The concomitant and exclusive appearance, in both the HT and LT suites of this region, of the hottest and deepest (T_p up to ~1590

°C and P up to ~5 GPa) high-MgO sub-lithospheric magmas ($^{87}Sr/^{86}Sr$ 0.70319-0.70533 and $\varepsilon Nd_{(t)}$ from 9.08 to 0.53) is consistent with their generation from the axial zone of the upwelling plume. The basic–acidic bimodal character of CFB magmatism, since the beginning of this stage, must be related to the intensive block faulting of the rifted margins that favoured magma trapping and crystal fractionation to trachydacite and dacite-rhyolite differentiates from the respective HT and LT basalts. Owing to the higher SiO_2 and viscosity, the prevailing dacite-rhyolite magmas were more prone to pond in crustal magma chambers, where they experienced assimilation fractional crystallisation ($^{87}Sr/^{86}Sr$ 0.71466-0.72558 and $\varepsilon Nd_{(t)}$ from −5.50 to −9.31) before erupting as extensive rheo-ignimbrites. During the final rifting stage, CFB activity continued until 128 Ma (with sporadic episodes until 122 Ma), and the plume dynamic support gradually vanished beneath the two conjugate South American/South African continental margins, up to the opening of the South Atlantic and hot-spot volcanism of the Rio Grande and Walvis Ridges.

Key words: Paranà-Etendeka, CFB, Plume-lithosphere interaction, magma differentiation

Introduction

Since the early work of Morgan (1971), a multidisciplinary debate has arisen regarding mantle plumes, mainly concerning their provenance, causative events, and relationships with hot spots, large igneous provinces (LIPs), and rift volcanism (Bercovici et al., 1989; White and McKenzie, 1989; Griffiths and Campbell, 1990; Ernst and Buchan, 2001; Tan et al., 2002; Courtillot et al., 2003; Davaille et al., 2005; Davies and Bunge, 2006; White, 2010; Beccaluva et al., 2011). The generation of continental flood basalts (CFB), characterised by large eruption rates, thermal anomalies, and focused regional uplift/rifting, was often attributed to the thermo-mechanical effects of rising hot mantle plumes (e.g., Richard et al., 1989; White and McKenzie, 1989; Arndt and Christensen, 1992; Ernst and Buchan, 2001; Campbell and Kerr, 2007; Natali et al., 2016; 2017), but alternative mechanisms include plate-driven melting related to the extensional lithosphere (e.g., Foulger et al., 2005; Foulger and Jurdy, 2007), and internal heating beneath continents (e.g., Coltice et al., 2009). Geochemical data (incompatible elements, and stable and radiogenic isotopes) have been used to establish the influence of the lithosphere (sub-continental lithospheric mantle) and/or plume related asthenospheric components in CFB magmas (Ellam and Cox, 1991; Ellam et al., 1992; Thomson et al., 2001; Herzberg and O'Hara, 2002; Campbell and Davis, 2006; Carlson et al., 2006; Hawkesworth and Schersten, 2007; Beccaluva et al., 2009; Zhang et al., 2010). CFBs generally range from low-TiO_2 (LT) to high-TiO_2 (HT) suites, with the latter often including high-MgO rocks (e.g. picrites and meimechites) that also record eclogite/pyroxenite components, which were recycled via ancient subduction and entrained by the rising plume from the transition zone or the lower mantle (Gibson et al., 2000; Tuff et al., 2005; Beccaluva et al., 2009; Sobolev et al., 2007 and 2009; Jackson and Carlson, 2011; Kamenetskey et al., 2012; Heinonen et al., 2013 and 2014; Rosenthal et al., 2014; Natali et al., 2016). Recently, systematic investigations by Natali et al. (2016; 2017) have shown that many Gondwana CFB provinces (e.g. Ethiopia-Yemen, Deccan, and Karoo) are compositionally zoned and characterised by the hottest and deepest HT picrite-basalts in the inner portion and LT in the periphery, with the former representing the most genuine proxies of plume-related magmas. Moreover, the Gondwana LIPs (including the Paranà-Etendeka) share the peculiar coexistence of alkaline/carbonatite complexes and picritic magmas at the intersection of regional extensional lineaments; this is a further indication that these areas represent the focus of the plume-related tectono-magmatic activities (Natali et al., 2018).

The Paranà-Etendeka LIP represents an unsolved puzzle, despite the large number of geological, geophysical, and geochemical studies published on it in the last 30 years. This is primarily due to the intrinsic complexity of this province, which is characterised by the strong tectono-magmatic asymmetry between its western and eastern parts on either margin of the South Atlantic: a) the Paranà plateau basalts of South America share similarities, e.g. LT and HT magma types and large erupted volumes with typical CFBs, except that their isotopic signatures demonstrate a prevalent contribution of lithospheric over asthenospheric source components; b) the Etendeka CFB magmatism of South West Africa is dominantly fissural, bimodal, and similar to that of rifted continental margins, except for the exclusive presence of high-MgO basalt-picrite suites that are more akin to sublithospheric plume-related melts. Moreover, although there is a consensus on the main magmatic activity during 135–130 Ma, the timing of the various events in the province and the duration of the main Paranà CFB are debated, thereby propagating uncertainties in any reconstruction of the tectonomagmatic evolution. Therefore, various hypotheses on the origin of the Paranà-Etendeka Province have been proposed, the most popular of which are related to either to 1) the activation of the proto-Tristan mantle plume (Cordani et al., 1980; White and McKenzie, 1989; 1995; Bizzi et al., 1995; Gibson et al., 1995; 2006; Thompson et al., 2001; Campbell, 2001; Ewart et al., 2004a; Tuff et al., 2005; Campbell and Davies, 2006), 2) the passive rifting events that mainly involved melting of the lithosphere under extension (Piccirillo and Melfi., 1988; Piccirillo et al., 1989, 1990; Comin Chiaramonti et al.,1997; Ernesto et al., 2002; Iacumin et al., 2003; Fairhead & Wilson, 2005; Rocha-Junior et al., 2013; Foulger.,2018), or 3) the lithospheric melting triggered by warming from an underlying mantle plume, provided that enough time for conductive heat transfer was available (Turner et al., 1994, 1996; Peate et al.,1990 and 1999; Hawkesworth et al., 1988, 1992 and 2000).

In our opinion, it is timely to carefully reconsider and homogeneously compare all the available data on the Paranà-Etendeka Province to verify whether it is possible to reconcile the different interpretations of its origin. For this purpose, we reviewed over 500 major, trace element and Sr-Nd-Pb isotopic analyses from the literature and reprocessed them to obtain homogeneous geochemical, petrological, and physical-chemical models (see Methods in the Electronic Appendix) for a comprehensive revaluation of:

1) the role of the "mantle plume" versus the "lithosphere" processes in the genesis of CFB from the Paranà to Etendeka regions;

2) the petrogenesis of the bimodal basalt-silicic rock associations, in both LT and HT suites, that represents a particularly debated event in the evolution of the province; and

3) a general model of a coherent tectonomagmatic scenario that fits the data, from the inception of plateau activity to rifting and continental breakup.

The Paranà-Etendeka CFB province

Magma types, spatial distribution and age

The Paranà-Etendeka CFB province represents an originally single LIP separated by the opening of the South Atlantic. It covers a total area of ~1.5 million km^2, of which ~ 95% is exposed in the Paranà region of South America, and the remaining portion is exposed in the Etendeka (Namibia) and Angola region along the south-western African coast. The magmatic products predominately consist of HT and LT basaltic suites in the Paranà Plateau, but become bimodal (mafic-felsic) from the south-eastern Paranà into the Etendeka, with silicic volcanics commonly occurring late in the sequences. The geochemical data reviewed in this work were used to update the paleogeographic reconstruction of the province, as illustrated in **Fig. 1**. Samples from the two suites were reclassified (Fig. 2), according to the total alkali-silica (TAS) and TiO_2 vs MgO diagram proposed by Natali et al. (2017) for Gondwana LIPs: 1) the LT tholeiitic suite exhibits lower alkali/silica ratios and includes basaltic to andesitic rocks (TiO_2 0.5–2.5 wt%) which are associated with dacite-rhyolite volcanics (TiO_2 0.6–1.2 wt%); 2) the HT tholeiitic suite shows comparatively higher alkali/silica ratios and includes basaltic to andesitic rocks (TiO_2 2.0–4.5 wt%) which are associated with trachydacite volcanics (TiO_2 1.0–1.6 wt%). In the Etendeka region, unlike the Paranà region, both suites include high-MgO basalts and picrites (MgO $\geq$ 13%), which are associated with olivine-rich gabbroic intrusives.

The largest part of the western province is represented by the Paranà plateau *s.s.* in Brazil (~800 000 km^3) and mainly consists of rather differentiated basalts ($\leq$ 8% MgO) that are HT (Paranapanema, Pitanga, and Urubici type localities) in the north-central part, and LT (Esmeralda and Gramado type localities) in the south (Bellieni et al., 1986; Piccirillo and Melfi, 1988; Piccirillo et al., 1989; 1990; Raposo et al., 2018). Along the south-eastern margin of the plateau, extensive LT dacite-rhyolite volcanics (Palmas-type) and minor HT trachydacite lavas (Chapeco-type) are associated with the respective LT and HT basaltic suites, exhibiting a total volume of ~20 000 km^3. Although Palmas-type lava domes and flows have been reported (e.g. Caxias do Sul dacites; Rossetti et al., 2018; Simões et al., 2019), the enormous LT silicic volcanic sheets of up to 400 m in thickness and extending for hundreds of kilometres have been interpreted as high temperature, low explosivity rheo-ingnimbrites (Bellieni et al., 1986; Garland et al., 1995; Bryan et al., 2010; Luchetti et al., 2018a; 2018b).

The regional lithospheric thickness beneath the Paranà Basin is $\geq$ 150 km, and the Moho depth is recorded at ~42 km (Snoke and James, 1997). The continental basement corresponds to a composite assemblage of Archean to early Proterozoic cratons (Sao Francisco and Rio de Plata) which are bordered by the Damara Pan-African Belt and fragmented along two main tectonic lineaments (NW-SE- and NE-SW-oriented), and whose reactivation in the Lower Cretaceous allowed for CFB fissural eruptions throughout the basin (Zalan et al., 1987; Piccirillo et al., 1990;

Gray et al., 2008; Licht, 2018 and references therein). These tectonic lineaments mainly crosscut in central Paranà, which corresponds to both the maximum thickness (~1700 m) of the HT basalts and the regional gravity high (Vidotti et al., 1998; Licht, 2018), thereby indicating that the focus of the plateau tectonomagmatic activity was in this area.

East of the Paranà Plateau *s.s.*, three main basaltic dyke swarms (DS) cut through the Brazilian coastal margin and radiate in various directions: the N-S Florianopolis DS, the NW-SE Ponta Grossa Arch DS, and the NE-SW Santos-Rio de Janeiro DS. Moreover, Buchan and Ernst (2019) emphasised the occurrence of giant circumferential dykes at right angles with the radiating dykes in the Ponta Grossa region, which are considered a characteristic of plume-related LIPs. In the paleogeographic reconstruction, the radiating extensional structures perfectly match the similarly oriented DS of the Etendeka-Angola margin and represent, overall, the site where the rifting processes developed and ultimately led to the continental breakup (Piccirillo et al., 1990; Raposo et al., 1998; Marzoli et al., 1999; Florisbal et al., 2018; Marsh and Swart, 2018).

In the African part of the province, CFB magmatism is clearly bimodal and consists of elongated volcanic and subvolcanic bodies and dike swarms that are set along the Etendeka/southern Angola costal margins across a total area of ≤ 100 000 km^2. A N-S spatial zonation, similar to that of the Paranà plateau, is observed for the HT basalt/trachydacites predominant in Angola and northern Etendeka (Khumib- and Doros-type localities), whereas the LT basalts/dacite-rhyolite rheo-ignimbrites prevail in southern Etendeka at the Tafelberg- and Horingbai-type localities (Erlank et al., 1984; Duncan et al., 1990; Milner et al., 1992, 1995 ; Milner and Le Roex, 1996; Peate et al., 1999; Marsh et al., 2001, Ewart et al., 2004a; 2004b; Marsh and Swart, 2018). In addition, the Etendeka HT and LT suites include high-MgO picrite-basalt lavas and dykes, which are sometimes associated with olivine-rich gabbroic rocks (Gibson et al., 2000; Thompson et al., 2001; Jennings et al., 2017; Owen-Smith et al,.2017). There is a clear and precise correlation between the basalt/dacite-rhyolite suites from Serra Geral (south-eastern Paranà) and those from the Etendeka margin. Therefore, these sectors have to be considered the uplifted rift shoulders of the South America/South Africa conjugate margins, and the area in between represents a triple point where the main DS converge (Milner et al., 1995; Marsh et al., 2001; Peat et al., 1999; Marsh and Swart, 2018; Florisbal et al., 2018; Buchan and Ernst, 2019).

The geochronology of the Paranà/Etendeka Province has been an object of debate, although there is a general agreement that most CFB erupted during 135–130 Ma (Stewart *et al.*, 1996; Renne *et al.*, 1996a; 1996b; Ernesto et al., 1999; Gibson *et al.*, 2006; Thiede and Vasconcelos, 2010; Janasi *et al.*, 2011; Pinto *et al.*, 2011). The duration of the Paranà Plateau activity has been controversial: it was considered to be *ca.* 10 Ma, (138–129/127 Ma), based on the laser spot total fusion for $^{40}Ar/^{39}Ar$ performed on the borehole of the thickest lava section (Stewart et al., 1994; Turner et al., 1994,1996; Mantovani et al., 1995), whereas the same samples re-analysed using laser incremental step heating (LISH) for Ar^{40}/Ar^{39} resulted in a much shorter time interval of 135–134 Ma (Thiede and Vasconcelos, 2010). The latter age range was confirmed by additional LISH Ar^{40}/Ar^{39} and U-Pb data on basalts and silicic volcanics at the south-eastern Paranà border (Licht et al., 2015; Pinto et al., 2011; Janasi et al., 2011). More recently, Baksi (2018) carried out new analyses and a severe selection of the available data, concluding that the most reliable LISH Ar^{40}/Ar^{39} and U-Pb datings indicate the beginning of the Paranà plateau CFB volcanism at ca. 135 Ma and a duration of ca. 1 Ma, which is also in agreement with the LISH Ar^{40}/Ar^{39} plateau ages of 135-134 Ma previously reported by Renne et al. (1992) for southern Paranà. This was also confirmed using U-Pb geochronology, Hf isotopes and trace element data indicating that zircon crystallisation in Paranà lavas occurred at ca. 134 Ma (Hartmann et al., 2019).

According to Ar^{40}/Ar^{39}, U-Pb, and magneto-stratigraphic data, the subsequent rifting stage, involving CFB fissural events from eastern Paranà plateau margin to Etendeka and southern Angola, climaxed during 134–130 Ma, and continued until 128–127 Ma (Renne et al., 1992; 1996a; 1996b; Milner et al., 1995; Stewart et al., 1996; Marzoli et al., 1999; Ernesto et al., 1999; Florisbal et al., 2014; Dodd et al., 2015; Owen-Smith et al., 2017), i.e. until the continental breakup was completed and the oldest South Atlantic oceanic crust formed at the same latitudes (Chron M4

126.5 Ma; Gradstein et al., 1994; Franke et al., 2010; Nurnberg and Muller, 1991). Sporadic basaltic dyke activity continued in the new conjugate South American and South African margins until c.a. 122 Ma (Raposo et al., 1998; Renne et al., 1996b).

A careful evaluation of the most statistically robust dating allows the timing of the rifting processes to be more precisely constrained. The agreement between most LISH Ar^{40}/Ar^{39} (134–132 Ma; Renne et al., 1996b) and U-Pb ages (134–133 Ma; Almeida et al., 2018) for Ponta Grossa dykes and those of Florianopolis dykes (U-Pb ca 134 Ma; Florisbal et al., 2014) suggests that the early rifting stage along the Brazilian margin mainly took place between 134 and 132 Ma (cf, Baksi, 2018). The LISH Ar^{40}/Ar^{39} dates for the main Etendeka sections consistently indicate that most of the CFB picrite-basalt-silicic events occurred in the time interval 132–130 Ma (Renne et al., 1996b; Owen-Smith et al., 2017). Therefore, the spatial-temporal evolution delineated above is in agreement with the eastward migration of the Paranà-Etendeka CFB volcanism (Melfi, 1967; Bellieni et al., 1984b; Fodor et al., 1989; Piccirillo et al., 1988; Mantovani et al., 1995) or, more precisely, from the NW (Paranà Plateau) to SE (Etendeka) in relation to the opposite drifting of the Gondwana lithosphere over the active proto-Tristan plume (O'Connor and Duncan, 1990; Turner et al., 1994; Stewart et al., 1996; Gibson et al., 2006).

Petrogenesis of HT and LT suites

The integration of multiple approaches, such as major element phase equilibria, trace element modelling, Sr-Nd-Pb isotopes, and thermobarometric estimates were utilised to constrain the P-T-X genetic conditions of CFB magmas and their differentiation processes. The identification of parental magmas and their liquid line of descent (LLD) is not straightforward because of the difficulties in evaluating the source composition, melting conditions, and the possible occurrence of mixing and cumulus processes of magmas that rise in a short time along the same feeding system. Therefore, these approaches were applied to test the inter-modelling best fit.

Basaltic rocks

One approach to identify the most primitive magmas is illustrated by the MgO-FeO diagram in **Fig. 3,** where the petrogenetic grid for the various CFB suites for the entire Paranà-Etendeka Province is reported together with the forsterite (Fo) theoretical composition of the coexisting olivine. Unlike Paranà rocks, Etendeka basalts include volcanic and subvolcanic picritic types having up to MgO 18 wt%, which denote cumulus olivine in some samples (labelled *c* in Fig. 3).

Starting from the least-differentiated HT and LT basalt-picrite compositions, the reconstruction of the primary melts and potential temperatures (T_p) was performed by iterative calculations of the fractional melting algorithm PRIMELT3MEGA (Herzberg and Asimow, 2015), and by using anhydrous lherzolite KR4003 as the mantle source (Walter, 1998). The resulting primary melts from Etendeka are, on average, comparatively richer in MgO and FeO than those of Paranà. This results in a systematically higher T_p (~1590 °C for HT and 1520 °C for LT) in Etendeka than in Paranà (1550 °C for HT and 1500 °C for LT). An even higher T_p (1623 °C) was proposed by Jennings et al (2019), based on the Al-in-olivine thermometry of Etendeka picrites. The estimated generation pressure for primary melts was approximately around 3–4 GPa according to Natali et al. (2018), but for Etendeka HT, it reached ~5 GPa. Overall, these data are in agreement with those reported for other Gondwana provinces, such as Ethiopia-Yemen, Deccan and Karoo, where CFB generation was triggered by the impinging of thermo-compositionally zoned plume heads with thermal anomalies of 250–300 °C relative to the ambient mantle (Natali et al. 2016; 2017;2018).

The chondrite-normalised rare earth element (REE) patterns of the basaltic rocks of the entire province (**Fig. 4)** display a systematic light REE (LREE) enrichment of HT with respect to the LT suites, with La_N/Yb_N ratios varying from 7.0–8.5 to 4.0–4.7, respectively. In principle, this may reflect either a lower degree of melting and/or a higher incompatible element enrichment of the HT mantle sources. More reliable petrogenetic constraints were obtained through melting modelling of HT and LT from Etendeka and Paranà as reported in the primitive mantle (PM)-normalised incompatible element diagrams (**Fig. 5).** Overall, magmas from the two regions are similar with respect to the heavy REE (HREE) + Y and high field strength elements (HFSE) such as Ti and Zr, but they are remarkably different for LREE and low FSE (LFSE) like K, Ba, and Th, which are significantly more enriched in Paranà. Accordingly, modelling the former group of elements is roughly compatible with that of PM sources for all magmas of the province, whereas the Paranà basalts require an appropriate LREE-LFSE enrichment in their sources. The incompatible element distribution of Paranà magmas compare favourably with that of the EM1 component (Weaver, 1991). This component is considered a common geochemical signature of the sub-continental lithosphere (Bianchini et al, 2014). Accordingly, the involvement of the sub-continental lithosphere in the CFB sources was invoked by several studies (Hawkesworth et al., 1983; Ellam and Cox, 1991; Menzies , 1992).

The distribution of the CFB Sr-Nd-Pb isotopes confirms a provinciality between Paranà and Etendeka (**Fig. 6).** In fact, most high-MgO CFB from Etendeka (HT and LT picrites and some basalts) cluster in the upper left of the $\varepsilon Nd_{(t)}$-$^{87}Sr/^{86}Sr_{(i)}$ diagram with isotopic ranges of $\varepsilon Nd_{(t)}$= +9.08– +0.53 and $^{87}Sr/^{86}Sr_{(i)}$=0.70319–0.70533 (**Fig. 6a**). This was attributed (Thompson *et al.*, 2001; Ewart et al., 2004a; Hoernle *et al.*, 2015; Owen-Smith *et al.*, 2017; Natali et al, 2018) to uncontaminated sub-lithospheric sources and conforms to the isotopic signatures of plume-related mantle components observed in other Gondwana CFB provinces, such as Ethiopia-Yemen and Deccan (Natali *et al* 2016, 2017). Coherently, Stroncik et al. (2017) reported high helium isotopes in Etendeka picrites where $^{3}He/^{4}He$ values > 26 R/RA, which is typical of deep seated undegassed mantle reservoirs. In contrast, a significant portion of both the HT and LT basalts from Paranà (where $^{87}Sr/^{86}Sr_{(i)}$ is 0.70483–0.70620 and $\varepsilon Nd_{(t)}$ is −1.27 to +5.78) clusters around the EM1 component, which likely reflects the significant involvement of the sub-continental lithosphere in their sources (Piccirillo et al.,1989; Turner et al., 1996; Peate et al., 1999; Marques et al., 1999; 2018; Natali et al., 2018). Moreover, the higher $^{87}Sr/^{86}Sr_{(i)}$ values (up to 0.7142) of many LT (MgO down to 4–5 wt%), from both Paranà and Etendeka, reflect the variable extent of continental crust contamination during differentiation. Although the range of assimilated rocks possibly includes high grade-metamorphic rocks such as migmatitic and granulite terrains (de Abreu Barbosa Araujo et al., 2019; Miranda et al., 2020), mixing modellings indicate upper crust components to be the favoured contaminant (Hoernle et al., 2015) and, more specifically, granitoid lithologies of the Proterozoic age (Marques et al., 2018). **Figure 6b** reports the Pb isotopic composition of the entire Paranà-Etendeka population, which ranges between 15.4–15.8 for $^{207}Pb/^{204}Pb$ and 17.1–19.8 for $^{206}Pb/^{204}Pb$. The high-MgO Etendeka CFB plot from 15.5–15.7 for $^{207}Pb/^{204}Pb$ and 17.6–18. for $^{206}Pb/^{204}Pb$ and partly overlaps with the CFB from Paranà that show EM1 mantle affinity. In contrast, the high $^{207}Pb/^{204}Pb$ of up to 15.7 and $^{206}Pb/^{204}Pb$ of up to 19.9 for several samples of both sub-provinces are attributable to the upper crust contamination trends delineated previously (Hoernle et al., 2015; Marques et al., 2018).

Silicic rocks

In contrast to basaltic rocks, the petrogenesis of silicic magmas, occurring from south-eastern Paranà to Etendeka, have been the object of a longstanding debate, leading to various interpretations: a) HT trachydacites and LT dacites-rhyolites have been considered to be partial melts of the crust or of the same underplated HT and LT basalts, with which they are associated in the field (Erlank *et al.*, 1984; Bellieni *et al.*, 1986; Milner, 1988; Whittingham, 1991); b) LT dacites-rhyolites have been considered the products of open-system assimilation fractional crystallisation (AFC) from LT basalts (Garland et *al.*, 1995; Ewart *et al.*, 2004b); and c) HT trachydacites have been considered to be derived through the partial melting of underplated HT basaltic rocks (Garland *et al.*, 1995).

The various petrogenetic hypotheses were tested in terms of the physical-chemical conditions of the magma evolution in the two suites. First, quantitative fractional crystallisation (FC) models were analysed using PELE and MELTS softwares (Ghiorso and Sack, 1995;

Boudreau, 1999), assuming several non-cumulative high-MgO (9–12 wt%) basalts, as the most representative parental magmas in each suite, to compare the theoretical liquids (and fractionated solids) with those observed in the volcanics (**Figs. 7 and 8**). The calculated and observed results agree in terms of chemical evolutionary trends, fractionating phases, crystallisation order, and temperatures (c.f., Bellieni et al.; 1986; Piccirillo et al.,1988; Garland et al., 1995, Thompson et al., 2001; Ewart et al., 2004a; 2004b; Keiding et al., 2013).

Therefore, the compositional constraints and thermodynamic equilibria indicate that the assumed parental magmas can produce the observed differentiates, namely the HT trachydacites and LT dacite-rhyolites, through the FC and removal of 22% and 22% olivine, 33% and 41% plagioclase, 16% and 17% clinopyroxene, followed by 5.0% and 3.5% Fe-Ti oxides, 0.4% and 0.2% apatite, 0.0% and 0.2% orthopyroxene, respectively, in a temperature range of 1300–900 °C. For both suites, the drastic precipitation of Fe-Ti oxides during advanced fractionation stages (MgO $\leq$ 4 wt%) resulted in a sudden increase in silica (SiO_2 from ~57 wt% to 63% wt%, the “Daly gap”) and a transition to silicic residual liquids whose mineral parageneses and temperatures of $\leq$ 1070 °C were in agreement with those of previous estimates (T= 1100–950 C°; Garland et al., 1995: Simoes et al., 2019). Therefore, the HT and LT suites do not markedly differ in terms of their fractionation processes, except for the higher degree of silica saturation in the LT magmas, which is also testified by the orthopyroxene appearance in their predicted and modal mineral assemblages. Thus, the extreme differentiates of the two suites, although corresponding to similar liquid fractions in the range of F 0.13–0.15, attain lower silica contents in the HT trachydacites (up to 68 wt%) than in the LT dacite-rhyolites (up to ~73 wt%) .

PM-normalised FC modelling for incompatible elements was also performed by PELE software for both suites and is reported in **Fig. 9** together with the Chondrite-normalised REE distribution. The calculated differentiates from the assumed parental basalts are in agreement with those of the observed composition of trachydacites and dacite-rhyolites, and they reflect the distinct enrichment of the incompatible elements of the two suites. The observed Ti and Sr negative anomalies are consistent with the fractionation of Fe-Ti oxides and plagioclase, respectively. **Figure 10** displays the distribution of the V and Cr compatible elements versus Zr for the HT and LT suites, with the theoretical trends of FC and batch melting (BM) models, beginning from the respective basaltic compositions. The results indicate that FC and removal of the mineral phases predicted by the major element modelling satisfactorily fit the composition of the trachydacites and dacite-rhyolites, whereas this is not the case for the partial melting, which invariably generates acidic melts with substantially higher V and Cr contents, as previously reported for analogous magmatic systems (Hanson, 1978; Peccerillo *et al*., 2003 and 2007). It may be concluded that FC is the favoured mechanism for the generation of both HT and LT acidic magmas with respect to partial melting of underplated CFB or other crustal compositions. The latter sources are discounted by the experimental melting of granitoid/metasedimentary systems that invariably produce significantly more Al_2O_3 and less K_2O and FeO than those observed in the Paranà-Etendeka silicic rocks (Beard and Lofgreen, 1989; Thy et al., 1990; Patino Douce and Johnston, 1991; Skjerlie and Johnston, 1993; Wolf and Wyllie,1994; Garland et al., 1995; Rapp and Watson, 1995).

Some relevant geochemical differences between the HT and LT differentiates are shown in **Fig. 11**, where the Sr-Nd and Pb isotopes of the trachydacites and dacite-rhyolites are compared with those of their respective HT and LT basalts. The HT basalts and trachydacites are isotopically homogeneous, confirming their comagmatic relationships. The LT suite, however, shows a continuous variation from the basalts to dacite-rhyolites, which are systematically higher in their $^{87}Sr/^{86}Sr$, $^{207}Pb/^{204}Pb$ and $^{206}Pb/^{204}Pb$ ratios. The latter compositions can be satisfactorily accounted for by the AFC processes, as suggested by Piccirillo et al. (1988), Garland et al. (1995), and Thompson et al., (2007), who estimated up to a 20% assimilation of continental components in crustal magma chambers for LT differentiates. A plausible explanation of why dacite-rhyolites, unlike trachydacites, are systematically more prone to be crustally contaminated **(Fig 12a)**, is because of their higher viscosity, which is expected in the more silica-rich LT differentiates**.** In fact, based on data by Polo et al., (2018) on Paranà silicic volcanics under variably hydrated conditions

(H_2O 0–2.5 wt%,), the modelled viscosities may attain 10^5–10^6 Pa s in rhyolites (SiO_2 of up to ~73 wt%) and 10^4 -10^5 Pa s in trachydacites (SiO_2 of up to ~68 wt%) that are at least 1 to 2 orders of magnitude higher in LT than in HT acidic rocks **(Fig 12b)**. These rheological differences may result in an easier ascent without ponding in the crust for the less viscous (generally uncontaminated) HT magmas that underwent continuous FC, in accordance with their intensive porhyric character, flow banding and limited amounts of lavas and dykes. In contrast, the comparatively higher viscosity of LT magmas favoured their trapping and ponding in shallow crustal chambers where they accumulated and most likely experienced AFC processes. This scenario can also satisfactorily account for the diverse volcanological features of rhyolite-dacite magmas, where high-grade rheo-ignimbrites prevail over lavas as massive rewelded sheets related to high density pyroclastic currents that are characterised by magma fragmentation and vary in behaviour from hydrodynamic to brittle (Luchetti et al., 2018a; 2018b)

Conclusions

The extensive review of multidisciplinary studies on the Paranà-Etendeka CFB Province in the last thirty years allowed for the construction of a coherent tectonomagmatic scenario that may reconcile the controversial views on the plume versus lithosphere roles and petrogenesis of the HT and LT CFB suites from the initial plateau activity to the rifting and continental breakup. This new perspective relies on the critical revision of geo-chronological data that allows the tectonomagmatic activity of the province to be sub-divided into in two main stages with diverse characteristics: 1) the Paranà Plateau *s.s.* stage, 135–134 Ma, and 2) the subsequent rifting stage, 134–128 Ma, which developed eastward, contiguous to the plateau, and gradually formed new South American and African continental margins. These stages are further discussed below and are sketched in **Figs. 13 a, b, and c.**

The **Paranà plateau *s.s.*** is comparable to other Gondwana CFB provinces (Natali *et al.*, 2017) not only regarding the type, extension and zonal arrangement of HT and LT suites but also the eruption rate (~ 0.8 km^3/a) and short duration, thus supporting the interpretation that a single event was triggered by a rising hot plume impinging on the central Paranà lithosphere (**Figs.13a and b**). The location of the plume impact beneath central Paranà is supported by the occurrence of the thickest sequence of HT basalts, the regional gravity high, and the low S-wave velocity anomaly recorded at ~300 km in depth in the area (Van Der Lee et.al., 2001). Moreover, the occurrence of several alkaline complexes from 145 Ma to 138 Ma (Gibson et al., 1995, 2005; Comin Chiaramonti et al., 1997; Gomes and Comin Chiaramonti, 2017) and tholeiitic dikes at ~138 Ma (Stewart et al., 1996), at the westernmost margin of Paranà plateau conforms to the scenario of a focalised lithospheric perturbation related to the plume impact in the 10 Ma prior to the CFB main event (135–134 Ma). This time interval is sufficient for the lowermost lithosphere to equilibrate conductive and advective (plume-related) heat contributions (Turner et al., 1996; McKenzie et al., 2005; Gibson et al., 2006), thus providing suitable conditions for the generation of Paranà CFB in the estimated ranges of P =3–4 GPa and T_p = 1500–1550 °C. The incompatible element modelling of the calculated primary magmas from Paranà provides constraints on the melting degree (from ~10% for HT to ~24% for LT) based on HREE and HFSE of a PM source, which however, must be significantly enriched in LREE and LFSE. Sr-Nd-Pb isotopes of the Paranà least-differentiated basalts show affinities with the EM1 component, which is in accordance with their derivation from lower lithospheric sources. A large portion of the Paranà basalts (particularly the LT ones) are displaced with anomalously high $^{87}Sr/^{86}Sr$ isotopic ratios that conform to variable degrees of crustal contamination that is in parallel with differentiation (MgO down to 4–5 wt%) during their ascent to the surface. At the end of this stage (ca. 134 Ma), the magmatic activity of the south-eastern marginal part of the Paranà Plateau became bimodal with the eruption of the trachydacites and dacite-rhyolites associated with the HT and LT basalts, respectively. Petrological modelling and isotopic data suggest that these silicic rocks may represent FC products in both suites, with the general tendency of the more viscous LT dacite-rhyolites to experience AFC processes in shallow crustal chambers, before erupting as extensive rheo-ignimbrites. As generally observed in the Gondwana LIPS, the eruption of large amounts of "rhyolitic" magmas appears to be related to the variation in the stress regime from the regional extension which characterise the CFB plateaus to localised continental rifting, accompanying magma trapping, and differentiation to acidic melts (Natali et al., 2011; 2017).

The **rifting stage** (134–128 Ma) developed in spatial/temporal continuity with the final phase (bimodal) of the Paranà Plateau and was characterised by the south-east migration of the tectonomagmatic activity from the Brazilian to Etendekan-Angolan costal margins. This appears to be a consequence of the generalised north-west lithospheric drift over the pre-existing plume, whose spatial/temporal track can be recognised in the radiating/circumferential dyke swarms of the Ponta Grossa Arch (134–132 Ma). Thus, the Etendeka region is a triple point where extensional lineaments converge and radiate in the NW, NS, and NE directions; while the Ponta Grossa DS represents an aborted rift arm, the rifting of the two latter directions lasted until *ca.* 128 Ma, accompanying the formation of the new South American/African continental margins, up to the South Atlantic opening (*ca.* 127 Ma). This evolution satisfactorily fits the models of White and McKenzie (1989) and Stewart et al. (1996) where the lithosphere, impinged by a hot plume (T_p > 1500°C), undergoes thermal weakening and thinning by a stretching (ß) factor of 2 to 5, ultimately leading to the continental breakup and oceanisation. Coherently, recent tomographic models indicate that the Angolan lithosphere was eroded by plume-related thermochemical processes linked to the Paranà-Etendeka LIP emplacement (Celli et al., 2020). This is also consistent with the progressive lithosphere arching and uplifting (as observed for the Serra Geral escarpment in Brazil and the south-west African margin) in relation to the adiabatic upwelling and dynamic support exerted by the plume. In terms of lithological compositions, the Etendeka Province is similar (including the N-S zonal arrangement) to that of the Paranà Plateau because it is mainly represented by HT basalts evolving into trachydacites in northern Etendeka/southern Angola, and LT basalts evolving into dacite-rhyolites in southern Etendeka. However, the style of magmatism is remarkably different, as it is characterised by much lower magma volumes than that of the Paranà Plateau, which are fed by fissural eruptions along the coastal margins over a total area of ~100 000 km ^{2} (eruption rate < 0.1 km^3/a). Furthermore, the exclusive occurrence in Etendeka of high-MgO basalts and picrites, which belong to both HT and LT suites, is a fundamental difference with respect to the Paranà Plateau. As stated by Natali et al. (2016, 2017, 2018) for the other Gondwana CFB provinces, these rocks represent the hottest and deepest (T_p of up to 1590 °C, and P of up to 5 GPa) asthenospheric magmas generated by melting within the axial zone of the plume, where the rapid rise of relatively undifferentiated magmas was permitted through a thinned and deeply rifted lithosphere. The high $^3He/^4He$ (> 26 R/RA) reported by Stroncik et al. (2017) is further complementary evidence for a deep-seated mantle plume that was involved in the high-MgO Etendeka magmatism. The Sr-Nd-Pb isotopic composition of Etendeka high-MgO rocks corresponds to an uncontaminated sub-lithospheric signature that is in agreement with the "Gough component", which is considered a marker of the proto-Tristan plume activity since ca. 132 Ma (Hoernle et al., 2015). This reconstruction can also satisfactorily explain the coexistence of high-MgO CFB and alkaline-carbonatitic complexes (e.g. Juquia, Jacupiranga and others, Beccaluva et al. 1992; 2017; Comin Chiaramonti and Gomes, 2017), whose generation in the lithosphere at P = 2–3 GPa and T_p = 1300–1400 °C was related to the same plume effects (Natali et al., 2018). In the final rifting stages, until 128 Ma, the plume effect gradually weakened, and the internal portion of the new conjugated continental margins subsided, leading to oceanisation (ca. 127 Ma) and the oldest hot spot volcanism of the Rio Grande Rise and Walvis Ridge (O'Connor and Duncan.,1990; Gallagher and Hawkesworth., 1994; Gassmöller et al., 2016). As an additional consideration, we suggest that the renewed magma production recorded in the Rio Grande Rise (up to 0.3 km^3/a; Gallagher and Hawkesworth., 1994) may be a consequence of the interaction between the intervening oceanic spreading and the mantle plume. From this view, the overall geodynamic evolution of the Paranà-Etendeka may be analogous to that of the Northern Atlantic Province, where the excess volcanism of Iceland represents one of the best examples of ocean ridge/plume interaction taking place after CFB magmatism and continental breakup (White and Mckenzie, 1989; White et al., 1995; Thordarson and Larsen, 2007 and references therein).

We can conclude that, although the mantle plume hypothesis represents the favoured explanation of many CFB provinces, the simplistic assignment of specific geochemical components to plume effects should be avoided; the Paranà-Etendeka case in particular demonstrates that the plume-related CFB magmatism appears to be influenced by the lithosphere in the beginning, whereas the role of the sublithospheric plume effects are predominant during the subsequent tectono-magmatic evolution of the province.

Acknowledgements

We are grateful to the Editor G. Shellnutt, R.E. Ernst and an anonymous referee for the very constructive criticism and suggestions that greatly improved the manuscript.

References

Almeida, V.V., Janasi, V.A., Heaman, L.M., Shaulis, B.J., Hollanda, M.H.B.M., Renne, P.R., 2018. Contemporaneous alkaline and tholeiitic magmatism in the Ponta Grossa Arch Paraná-Etendeka Magmatic Province: constraints from U-Pb zircon/baddeleyite and $^{40}Ar/^{39}Ar$ phlogopite dating of the José Fernandes Gabbro and mafic dikes. Journal of Volcanology and Geothermal Resources 355, 55-65.

Arndt, N.T., Christensen U., 1992. The role of lithospheric mantle in continental flood volcanism: thermal and geochemical constraints. Journal of Geophysical Research 97, 10967-10981.

Baksi, A.K., 2018. Paraná flood basalt volcanism primarily limited to ~ 1 Myr beginning at 135 Ma: new 40Ar/39Ar ages for rocks from Rio Grande do Sul, and critical evaluation of published radiometric data. Journal of Volcanology and Geothermal Resources 355, 66–77.

Beard, J. S., Lofgren, G.E., 1989. Effects of water on the composition of partial melts of greenstone and amphibolite. Science 244, 195–197.

Beccaluva, L., Azzouni-Sekkal, A., Benhallou, A., Bianchini, G., Ellam, R.M., Marzola, M., Siena, F., Stuart, F.M., 2007. Intracratonic asthenosphere upwelling and lithosphere rejuvenation beneath the Hoggar swell (Algeria): evidence from HIMU metasomatised lherzolite mantle xenoliths. Earth and Planetary Science Letters 260, 482–494.

Beccaluva, L., Bianchini, G., Ellam, R.M., Marzola, M., Oun, K.M., Siena, F., Stuart, F.M., 2008. The role of HIMU metasomatic components in the African lithospheric mantle: petro- logical evidence from the Gharyan peridotite xenoliths, NW Libya. Geological Society of London, Special Publication 293, 253–277.

Beccaluva, L., Bianchini, G., Natali, C., Siena, F., 2009. Continental flood basalts and mantle plumes: a case study of the northern Ethiopian Plateau. Journal of Petrology 50, 1377–1403.

Beccaluva, L., Bianchini, G., Wilson, M., 2011. Volcanism and evolution of the African Lithosphere. Geological Society of America, Special Paper 478 (331 pp.)

Bellieni, G., Comin-Chiaramonti, P., Marques, L.S., Melfi, A.J., Nardy, A.J.R., Papatrechas, C., Piccirillo, E.M., Roisenberg, A., 1986. Petrogenetic aspects of acid and basaltic lavas from the Paranà plateau (Brazil): geological, mineralogical and petrochemical relationships. Journal of Petrology 27, 915–944.

Bellieni, G., Comin-Chiaramonti, P., Marques, L.S., Melfi, A.J., Piccirillo, E.M., Stolfa, D., 1984. Low-pressure evolution of basalt sills from bore-holes in the Paraná basin (Brazil). Tschermaks mineralogische und petrographische 33, 25–47.

Bercovici, D., Schubert, G., Glatzmaier, G.A., Zebib, A., 1989. Three-dimensional thermal convection in a spherical shell. Journal of Fluid Mechanics 206, 75–104.

Bianchini, G., Bryce, J.G., Blichert-Toft, J., Beccaluva, L., Natali, C., 2014. Mantle dynamics and secular variations beneath the East African Rift: Insights from peridotite xenoliths (Mega, Ethiopia). Chemical Geology 386, 49–58.

Bryan, S.E., Ukstins Peate, I., Peate, D.W., Self, S., Jerram, D.A., Mawby, M.R., Marsh, J.S., Miller, J.A., 2010. The largest volcanic eruptions on Earth. Earth-Science Reviews 102, 207-229.

Bizzi, L.A., De Wit, M.J., Smith, C.B., McDonald, I., Armstrong, R.A., 1995. Heterogeneous enriched mantle materials and Dupal-type magmatism along the SW margin of the São Francisco craton. Brazilian Journal of Geodynamics 20, 469–491.

Boudreau, A.E., 1999. PELE - a version of the MELTS software program for the PC platform. Computer & Geosciences 25, 21–203.

Buchan , K.L., Ernst, R.E., 2019. Giant Circumferential Dyke Swarms: Catalogue and Characteristics. In Srivastava R.K., Ernst R.E., Peng P. (eds.) Dyke Swarms of the World: A Modern Perspective, 1-44. Springer Geology.

Campbell, I., Kerr, A., 2007. The Great Plume Debate: Testing the plume theory. Chemical Geology 241, 149-152.

Campbell, I.H., 2001. Identification of ancient mantle plumes. Geological Society of America (GSA) Special Paper 352, 5–21.

Campbell, I.H., Davies, G.F., 2006. Do mantle plumes exist? Episodes 29, 162–168.

Carlson, R.W., Czamanske, G., Fedorenko, V., Ilupin, I., 2006. A comparison of Siberian Meimechites and kimberlites: implications for the source of high-Mg alkalic magmas and flood basalts. Geochemistry, Geophysics, Geosystems 7, Q11014.

Celli, N.l., Lebedev, S., Schaeffer, A.J., Gaina, C. 2020. African cratonic lithosphere carved by mantle mantle plumes. Nature Communications 11, 92.

Cernuschi, F., Dilles, J.H., Kent, A.J.R., Schroer, G., Raab, A.K., Conti, B., Muzio, R., 2015.Geology, geochemistry and geochronology of the Cretaceous Lascano East intrusive complex and magmatic evolution of the Laguna Merìn basin, Uruguay. Gondwana Research 28, 837–857.

Coltice, N., Bertrand, H., Rey, P., Jourdan, F., Phillips, B.R., Ricard, Y., 2009. Global warming of the mantle beneath continents back to the Archaean. Gondwana Research 15, 254–266.

Comin-Chiaramonti, P., Cundari, A., Piccirillo, E.M., Gomes, C.B., Castorina, F., Censi, P., De Min A., Marzoli A., Petrini R., Speziale S., Velázquez, V.F., 1997. Potassic and sodic igneous rocks from Eastern Paraguay: their origin from a lithospheric mantle and genetic relationships with the associated Paraná flood tholeiites. Journal of Petrology 38, 495-528.

Comin-Chiaramonti, P., Marzoli, A., Gomes, C.B., Milan, A., Riccomini, C., Mantovani, M.M.S., Renne, P., Tassinari, C.C.G., Vasconcelos, P.M., 2007. Origin of post Paleozoic magmatism in Eastern Paraguay. Geological Society of America (GSA) Special Paper 430, 603–633.

Cordani, U.G., Sartori, P.L., Kawashita, K., 1980. Geoquímica dos isótopos de estrôncio e a evolução da atividade vulcânica na Bacia do Paraná (Sul do Brasil) durante o Cretáceo. Anais da Academia Brasileira de Ciências 52, 811-818.

Courtillot, V., Davaille, A., Besse, J., Stock, J., 2003. Three distinct types of hotspots in the Earth's mantle. Earth and Planetary Science Letters 205, 295–308.

Danyushevsky, L.V., Plechov, V., 2011. Petrolog3: integrated software for modeling crystallization processes. Geochemistry, Geophysics, Geosystems 12. https://doi.org/10.1029/2011GC003516.

Davaille, A., Stutzmann, E., Silveira, G., Besse, J., Courtillot, V., 2005. Convective patterns under the Indo-Atlantic 'box'. Earth and Planetary Science Letters 239, 233–252.

Davies, J. H., Bunge, H-P., 2006. Are splash plumes the origin of minor hotspots?, Geology 34, 349-352.

Dessai, A.G., Markwick, A., Vaselli, O., Downes, H., 2004. Granulite and pyroxenite xenoliths from the Deccan Trap. Insight into the nature and composition of the lower lithosphere beneath cratonic India. Lithos 78, 263–290.

Dodd, S.C., Mac Niocaill, C., Muxworthy ,A.R., 2015. Long duration (>4 Ma) and steady-state volcanic activity in the early Cretaceous Paraná–Etendeka Large Igneous Province: New palaeomagnetic data from Namibia. Earth and Planetary Science Letters 414, 16–29.

Duncan, A.R., Armstrong, R.A., Erlank, A.J., Marsh, J.S., Watkins, R.T., 1990. MORB-related dolerites associated with the final phases of Karoo flood basalt volcanism in Southern Africa. In: Parker, A. J., Rickwood, P. C. & Hunter, D. H. (eds) Mafic Dykes and Emplacement Mechanisms. Rotterdam: Balkema, pp. 119–129.

Ellam, R.M., Carlson, R.W., Shirey, S.B., 1992. Evidence from Re–Os isotopes for plume lithosphere mixing in Karoo flood basalt genesis. Nature 359, 718–721.

Ellam, R.M., Cox, K.G., 1991. An interpretation of Karoo picrite basalts in terms of interaction between asthenospheric magmas and the mantle lithosphere. Earth and Planetary Science Letters 105, 330–342.

Erlank, A.J., Marsh, J.S., Duncan, A.R., Miller, R.M., Hawkesworth, C.J., Betton, P.J., Rex, D.C., 1984. Geochemistry and petrogenesis of the Etendeka volcanic rocks from South West Africa Namibia, Geological Society of South Africa Special Publication 13, 195–246.

Ernesto, M., Marques, L.S., Piccirillo, E.M., Molina, E.C., Ussami, N., Comin-Chiaramonti, P., Bellieni, G., 2002. Paraná Magmatic Province-Tristan da Cunha plume system: fixed versus mobile plume, petrogenetic considerations and alternative heat sources. Journal of Volcanology and Geothermal Research 118, 15–36.

Ernesto, M., Raposo, M.I.B., Marques, L.S., Renne, P.R., Diogo, L.A., de Min, A., 1999. Paleomagnetism, geochemistry and 40Ar/39Ar dating of the north-eastern Paraná Magmatic Province: Tectonic implications: Journal of Geodynamics 28, 321–340.

Ernst, R.E., Buchan, K.L., 2001a. Mantle plumes: their identification through time. Geological Society of America (GSA) Special Paper 352, 593 pp.

Ewart, A., Marsh, J.S., Milner, S.C., Duncan, A.R., Kamber, B.S., Armstrong, R.A., 2004a. Petrology and Geochemistry of Early Cretaceous Bimodal Continental Flood Volcanism of the NW Etendeka, Namibia. Part 1: Introduction, Mafic Lavas and Re-evaluation of Mantle Source Components. Journal of Petrology 45, 59-105.

Ewart, A., Marsh, J.S., Milner, S.C., Duncan, A.R., Kamber, B.S., Armstrong, R.A., 2004b. Petrology and Geochemistry of Early Cretaceous Bimodal Continental Flood Volcanism of the NW Etendeka, Namibia. Part 2: Characteristics and Petrogenesis of the High-Ti Latite and High-Ti and Low-Ti Voluminous Quartz Latite Eruptives. Journal of Petrology 45, 107-138.

de Abreu Barbosa Araujo, L.E. Heilbron, M., de Morisson Valeriano, C., Teixtera, W., Aguiar Neto, C.C., 2019. Lithogeochemical and Nd-Sr isotope data of the orthogranulites of the Juiz de Fora complex, SE-Brazil: insights from a hidden Rhyacian Orogen within the Ribeira belt. Brazilian Journal of Geology. vol.49, no3, e20190007.

Fairhead, J. D., Wilson, B. M., 2005. Plate tectonic processes in the South Atlantic Ocean: Do we need deep mantle plumes?, Geological Society of America (GSA) Special Paper 388, 537–553.

Florisbal, L.M., Janasi, V.A., Bitencourt, M.F., Nardi, L.V.S., Marteleto, N.S., 2018. Geological, geochemical and isotope diversity of~ 134 Ma dykes from the Florianópolis Dyke Swarm, Paraná Magmatic Province: Geodynamic controls on petrogenesis. Journal of Volcanology and Geothermal Research 355, 181-203.

Florisbal, L.M., Heaman, L.M., Janasi, V.A., Bitencourt, M.F., 2014. Tectonic significance of the Florianópolis Dyke Swarm, Paraná-Etendeka Magmatic Province: a reappraisal based on precise U-Pb dating. Journal of Volcanology and Geothermal Research 289, 140–150.

Fodor, R.V., Mckee, E.H., Roisenberg, A., 1989. Age distribution of Serra Geral (Paraná) flood basalts, southern Brazil. Journal of South American Earth Sciences 2, 343-349.

Fodor, R.V., Sial, A.N., Gandhok, G., 2002. Petrology of spinel peridotite xenoliths from northeastern Brazil: lithosphere with a high geothermal gradient imparted by Fernando de Noronha plume. Journal of South American Earth Sciences 15, 199–214.

Foulger, G.R., 2018. Origin of the South Atlantic Igneous Province. Journal of Volcanology and Geothermal Research 355, 2–20.

Foulger, G.R., Jurdy, D.M., 2007. Plates, plumes and planetary processes. Geological Society of America (GSA) Special Paper 430, 997 pp.

Foulger, G.R., Natland, J.H., Presnall, D.C., Anderson, D.L., 2005. Plates, plumes and paradigms. Geological Society of America (GSA) Special Paper 388, 881 pp.

Franke, D., Ladage, S., Schnabel, M., Schreckenberger, B., Reichert, C., Hinz, K., Paterlini, M., de Abelleyra, J., Siciliano, M., 2010. Birth of a volcanic margin off Argentina, South Atlantic. Geochemistry Geophysics Geosystems 11, Q0AB04.

Garland, F., Hawkesworth C.J., Mantovani, M.S.M., 1995. Description and petrogenesis of the Paraná Rhyolites, Southern Brazil. Journal of Petrology 36, 1193–1227.

Gassmöller, R., Dannberg, J., Bredow, E., Steinberger, B., Torsvik, T. H., 2016. Major influence of plume-ridge interaction, lithosphere thickness variations, and global mantle flow on hotspot volcanism—The example of Tristan. Geochemistry Geophysics Geosystems 17, 1454–1479.

Ghiorso, M.S., Sack, R.O., 1995. Chemical mass transfer in magmatic processes, IV, A revised and internally consistent thermodynamic model for the interpolation and extrapolation of liquid-solid equilibria in magmatic systems at elevated temperatures and pressures. Contributions to Mineralogy and Petrology 119, 197–212.

Gibson, S.A., Thompson, R.N., Day, J.A., 2006. Timescales and mechanisms of plume-lithosphere interactions: 40Ar/39Ar geochronology and geochemistry of alkaline igneous rocks from the Paraná-Etendeka large igneous province. Earth and Planetary Science Letters 251, 1–17.

Gibson, S.A., Thompson, R.N., Day, J.A., Humphris, S.E., Dickin, A.P., 2005. Melt-generation processes associated with the Tristan mantle plume: Constraints on the origin of EM-1, Earth and Planetary Science Letters 237, 744–767.

Gibson, S.A., Thompson, R.N., Dickin, A.P., 2000. Ferropicrites: geochemical evidence for Fe-rich streaks in upwelling mantle plumes. Earth and Planetary Science Letters 174, 355–374.

Gibson, S.A., Thompson, R.N., Dickin, A.P., Leonardos, O.H., 1995. High-Ti and low-Ti mafic potassic magmas: key to plume-lithosphere interactions and continental flood-basalt genesis. Earth and Planetary Science Letters 136, 149–165.

Giordano, D., Russell, J.K., Dingwell, D.B., 2008. Viscosity of Magmatic Liquids: A Model. Earth and Planetary Science Letters 271,123-134.

Gomes C.B., Comin-Chiaramonti P., 2017. Magmatismo alcalino continental da região meridional da Plataforma Brasileira. São Paulo, Edusp/Fapesp, 608 p.

Gonnermann, H.M., Manga, M., 2012. Dynamics of magma ascent in the volcanic conduit.

Modeling Volcanic Processes. In: Fagents, S.A., Gregg, T.K.P., Lopes, R.M.C. (eds), The Physics and Mathematics of Volcanism, pp. 55-84.

Gradstein, F.M., Ogg, J.G., and Smith, A.G., 2004, A geologic time scale 2004: Cambridge, Cambridge University Press, 610 pp.

Gray, D.R., Foster, D.A., Meert, J.G., Goscombe, B.D., Armstrong, R., Trouw, R.A.J., Passchier, C.W., 2008. A Damara orogen perspective on the assembly of southwestern Gondwana. In: Pankhurst, R.J., Trouw, R.A.J., Brito Neves, B.B., De Wit, M.J. (eds), West Gondwana: pre-cenozoic correlations across the South Atlantic Region. Geological Society of London, Special Publications 294, pp 399–412.

Griffin, W.L., O'Reilly, S.Y., Natapov, L.M., Ryan, C.G., 2003. The evolution of lithospheric mantle beneath the Kalahari Craton and its margins. Lithos 71, 215–241.

Griffiths, R. W., Campbell, I. H., 1990. Stirring and structure in mantle starting plumes. Earth and Planetary Science Letters 99, 66–78.

Hanson, 1978. The application of trace element to the petrogenesis of igneous rocks of granitic composition. Earth and Planetary Science Letters 38, 26-43.

Hartmann, L.A., Baggio, S.B., Bruckmann, M.T., Knijnik, D.B., Lana, C., Massone, H.-J., Opitz, J., Pinto, V.M., Sato, K., Tassinari, C.C.G., Arena, K.R., 2019. U-Pb geochronology of Paranà volcanics combined with trace element geochemistry of the zircon crystals and zircon Hf isotope data. Journal of South American Earth Sciences 89, 219-226.

Hawkesworth, C.J., Marlow, A.G., 1983. Isotope evolution of the Damara Orogenic Belt. In: Miller, R.McG. (ed), Evolution of the Damara orogen of South West Africa/Namibia. Geological Society of South Africa Special Publication 11, pp. 397-407.

Hawkesworth, C.J., Gallagher, K., Kelley, S., Mantovani, M., Peate, D.W., Regelous, M., Rogers, N.W., 1992. Paraná magmatism and the opening of the South Atlantic. London Geological Society (GSL) Special Publications 68, 221-240.

Hawkesworth, C.J., Gallagher, K., Kirstein, L., Mantovani, M.S.M., Peate, D.W., Turner, S., 2000. Tectonic controls on magmatism associated with continental break-up: an ex- ample from the Paraná–Etendeka Province. Earth and Planetary Science Letters 179, 335–349.

Hawkesworth, C., Schrestén, A., 2007. Mantle plumes and Geochemistry. Chemical Geology 241, 319-331.

Heinonen, J.S., Carlson, R.W., Riley, T.R., Luttinen, A.V., Horan, M.F., 2014. Subduction-modified oceanic crust mixed with a depleted mantle reservoir in the sources of the Karoo continental flood basalt province. Earth and Planetary Science Letters 394, 229–241.

Heinonen, J.S., Luttinen, A.V., Riley, T.R., Michallik, R.M., 2013. Mixed pyroxenite– peridotite sources for mafic and ultramafic dikes from the Antarctic segment of the Karoo continental flood basalt province. Lithos 177, 366–380.

Herzberg, C., Asimow, P.D., 2015. PRIMELT3MEGA.XLSM software for primary magma calculation: Peridotite primary magma MgO contents from the liquidus to the solidus. Geochemistry, Geophysics, Geosystems 8. https://doi.org/10.1002/2014GC005631.

Herzberg, C., O'Hara, M.J., 2002. Plume associated magmas of Phanerozoic age. Journal of Petrology 43, 1857–1883.

Hoernle, K., Rohde, J., Hauff, F., Garbe-Schönberg, D., Homrighausen, S., Werner, R., Morgan, J.P., 2015. How and when plume zonation appeared during the 132 Myr evolution of the Tristan hotspot. Nature Communications 6, 7799.

Iacumin, M., De Min, A., Piccirillo, E.M., Bellieni, G., 2003. Source mantle heterogeneity and its role in the genesis of Late Archean-Proterozoic (2.7–1.0 Ga) and Mesozoic (200 and 130 Ma) tholeiitic magmatism in the south American Platform. Earth-Science Reviews 62, 365–397.

Jackson, M.G., Carlson, R., 2011. An ancient recipe for flood basalt genesis. Nature 476, 316–319.

Janasi, V.A., Freitas, V.A., Heaman, L.H., 2011. The onset of flood volcanism, Northern Paraná Basin, Brazil: a precise U-Pb baddeleyite/zircon age for a Chapecó-type dacite. Earth and Planetary Science Letters 302, 147–153.

Jennings, E.S., Gibson, S.A., Maclennan, J., 2019. Hot primary melts and mantle source for the Paraná-Etendeka flood basalt province: new constraints from Al-in-olivine thermometry. Chemical Geology 529, 119287.

Jennings, E.S., Gibson, S.A., Maclennan, J., Heinonen, J.S., 2017. Deep mixing of mantle melts beneath continental flood basalt provinces: constraints from olivine- hosted melt inclusions in primitive magmas. Geochimica et Cosmochimica Acta 196, 36–57.

Kamenetsky, V.S., Chung, S.-L., Kamenetsky, M.B., Kuzmin, D.V., 2012. Picrites from the Emeishan Large Igneous Province, SWChina: a compositional continuum in primitive magmas and respective mantle sources. Journal of Petrology 53, 2095–2113.

Karmalkar, N.R., Duraiswami, R.A., Chalapathi Rao, N.V., Paul, D.K., 2009. Mantle-derived mafic-ultramafic xenoliths and the nature of Indian sub-continental lithosphere. Journal of the Geological Society of India 73, 657–679.

Keiding, J.K., Frei, O., Renno, A.D., Veksler, I.V., Trumbull, R.B., 2013. Conditions of magma crystallization in the Henties Bay-Outjo dyke swarm, Namibia: implications for the feeder system of continental flood basalts. Lithos 179, 16-27.

Licht, O.A.B., 2018. A revised chemo-chrono-stratigraphic 4-D model for the extrusive rocks of the Paraná Igneous Province. Journal of Volcanology and Geothermal Research 355, 32-54.

Licht, O.A.B., Valore, L.A., Szatmari, P., 2015. Faciology and stratigraphy of a Mafic Volcaniclastic Deposit (MVD), Serra Geral Group, Saudade do Iguaçu-Coronel Vivida region, State of Paraná, Brazil. Proceedings of VI Simpósio de Vulcanismo e Ambientes Associados, p. 49

Luchetti, A.C.F., Gravley, D.M., Gualda, G.A.R., Nardy, A.J.R., 2018a. Textural evidence for high-grade ignimbrites formed by low-explosivity eruptions, Paraná Magmatic Province, southern Brazil. Journal of Volcanology and Geothermal Research 355, 87–97.

Luchetti, A.C.F., Nardy, A.J.R., Madeira, J., 2018b. Silicic, high- to extremely high-grade ignimbrites and associated deposits from the Paraná Magmatic Province, southern Brazil. Journal of Volcanology and Geothermal Research 355, 270–286.

Lustrino, M., Melluso, L., Brotzu, P., Gomes, C.B., Morbidelli, L., Muzio, R., Ruberti, E., Tassinari, C.C.G., 2005. Petrogenesis of the early Cretaceous Valle Chico igneous complex (SE Uruguay): relationship with Paraná–Etendeka magmatism. Lithos 82,407–434.

Mahood, G.A., Stimac, J.A., 1990. Trace-element partitioning in pantellerites and trachytes. Geochimica et Cosmochimica Acta 54, 2257-2276.

Mantovani, M., Stewart, K., Turner, S., Hawkeswart, C.J., 1995. Duration of Paraná Magmatism and Implications for the evolution and source regions of continental flood basalts. Anais da Academia Brasileira de Ciências, 67, 163-169.

Marques, L.S., Duprè, B., Piccirillo, E.M., 1999. Mantle source compositions of the Paraná Magmatic Province (southern Brazil): evidence from trace element and Sr-Nd-Pb isotope geochemistry. Journal of Geodynamics 28, 439-458.

Marques, L.S., De Min, A., Rocha-Júnior, E.R.V., Babinski, M., Bellieni, G., Figueiredo, A.M.G., 2018. Elemental and Sr-Nd-Pb isotope geochemistry of the Florianópolis DykeSwarm (Paraná Magmatic Province): crustal contamination and mantlesource constraints. Journal of Volcanology and Geothermal Research 355, 149-164.

Marsh, J.S., Swart, R., 2018. The Bero Volcanic Complex: Extension of the Paraná-Etendeka Igneous Province into SW Angola. Journal of Volcanology and Geothermal Research, 355, 21-31.

Marsh, J.S., Ewart, A., Milner, S.C., Duncan, A.R., Miller, R.McG., 2001. The Etendeka igneous province: magma types and their stratigraphic distribution with implications for the evolution of the Paraná–Etendeka flood basalt province. Bulletin of Volcanology 62, 464–486.

Marzoli, A., Renne, P.R., Piccirillo, E.M., Ernesto, M., Bellieni, G., De Min, A., 1999. Extensive 200-million-year-old continental flood basalts of the Central Atlantic magmatic province. Science 284, 616–618.

Melfi, A.J., 1967. Potassium-argon dates for core samples of basaltic rocks from southern Brazil. Geochimica et Cosmochimica Acta 31, 1079–1089.

Menzies, M.A., 1992. The lower lithosphere as a major source for continental flood basalts: a re-appraisal. London Geological Society, Special Publications 68, 31-39.

Milner, S.C., le Roex, A.P., 1996. Isotope characteristics of the Okenyenya igneous complex, northwestern Namibia: constraints on the composition of the early Tristan plume and the origin of the EM1 mantle component. Earth and Planetary Science Letters 141, 277–291.

Milner, S.C., le Roex, A.P., O'Connor, J.M., 1995. Age of Mesozoic rocks in northwestern Namibia, and their relationship to continental breakup. Journal of the London Geological Society 152, 97–104.

Milner, S.C., Duncan, A.R., Ewart A., 1992.Quartz latite rheoignimbrite flows of the Etendeka Formation, north-western Namibia. Bulletin of Volcanology 54, 200-219.

Miranda, D.A., de Oliveira Chaves A., Dussin I.A., Porcher, C.C., Paleoproterozoic khondalites in Brazil: a case study of metamorphism and anatexis in khondalites from Itapecerica supracrustal succession of the southern São Francisco Craton. International Geology Review, doi.org/10.1080/00206814.2020.1716273.

Morgan, W.J., 1971. Convection in the lower mantle. Nature 230, 42-43.

Milner, S.C., 1988. The geology and geochemistry of the Etendeka Formation quartz latites, Namibia. Ph.D. Thesis, Univ. Cape Town, 263 pp.

Namiki, A., Manga, M., 2008. Transition between fragmentation and permeable outgassing of low viscosity magmas, Journal of Volcanology and Geothermal Research 169, 48–60.

Natali, C., Beccaluva, L., Bianchini, G., Siena, F., 2011. Rhyolites associated to Ethiopian CFB: clues for initial rifting at the Afar plume axis. Earth and Planetary Science Letters 312, 59–68.

Natali, C., Beccaluva, G., Bianchini, G., Ellam, R.M., Siena, F., Stuart, F., 2013. Carbonated alkali-silicate metasomatism in the North Africa lithosphere: evidence from Middle Atlas spinel-lherzolites, Morocco. Journal of South American Earth Sciences 41,113–121.

Natali, C., Beccaluva, G., Bianchini, G., Ellam, R.M., Savo, A., Siena, F., Stuart, F.M., 2016. High-MgO lavas associated to CFB as indicators of plume-related thermochemical effects: the case of ultra-titaniferous picrite–basalt from the Northern Ethiopian– Yemeni Plateau. Gondwana Research 34, 29–48.

Natali, C., Beccaluva, G., Bianchini, G., Siena, F., 2017. Comparison among Ethiopia-Yemen, Deccan, and Karoo continental flood basalts of central Gondwana: insights on lithosphere versus asthenosphere contributions in compositionally zoned magmatic provinces. Geological Society of America (GSA) Special Paper 526, 191–215.

Natali C., Beccaluva L., Bianchini, G., Siena, F. 2018. Coexistence of alkaline-carbonatite complexes and high-MgO CFB in the Paranà-Etendeka province: Insights on plume-lithosphere interactions in the Gondwana realm. Lithos, 296-299, 54-66.

Nürnberg, D., Müller, R.D., 1991. The tectonic evolution of the South Atlantic from Late Jurassic to present. Tectonophysics 191, 27-53.

O'Connor, M., Duncan, R.A., 1990. Evolution of the Walvis Ridge-Rio Grande Rise hot spot system: implications for African and South American plate motions over plumes. Journal of Geophysical Research 95, 17475-17502.

Owen-Smith, T.M., Ashwal, L.D., Sudo, M., Trumbull, R., 2017. Age and petrogenesis of the Doros Complex, Namibia, and implications for early plume-derived melts in the Paraná–Etendeka LIP. Journal of Petrology 58, 423–442.

Patiño Douce, A.E., Johnston, A.D., 1991. Phase equilibria and melt productivity in the pelitic system: implications for the origin of peraluminous granitoids and aluminous granulites. Contributions to Mineralogy and Petrology 107, 202–218.

Peate, D.W., Hawkesworth, C.J., Mantovani, M.S.M., Rogers, N.W., Turner, S.P., 1999. Petrogenesis and stratigraphy of the high-Ti/Y Urubici magma type in the Paraná flood basalt province and implications for the nature of 'Dupal'-type mantle in the South Atlantic region. Journal of Petrology 40, 451–473.

Peate, D.W., Hawkesworth J.C., Mantovani, S.M., Shukowsky, W. 1991. Mantle plumes and flood basalt stratigraphy in the Parana, South America. Geology 18, 1223-1226.

Peccerillo, A., Donati, C., Santo, A.P., Orlando, A., Yirgu, G., Ayalew, D., 2007. Petrogenesis of silicic peralkaline rocks in the Ethiopian rift: Geochemical evidence and volcanological implications. Journal of African Earth Sciences 48, 161–173.

Peccerillo, A., Barberio, M.R., Yurgu, G., Ayalew, D., Barbieri, M., Wu, T.W., 2003. Relationships between mafic and peralkaline silicic magmatism in continental rift settings: a petrological, geochemical and isotopic study of the Gedemsa volcano, central Ethiopian Rift. Journal of Petrology 44, 2003–2032.

Piccirillo, E.M., Bellieni, G., Cavazzini, G., Comin-Chiaramonti, P., Petrini, R., Melfi, A.J., Pinese, J.P.P., Zantadeschi, P., De Min, A., 1990. Lower Cretaceous tholeiitic dyke swarms from the Ponta Grossa arch (southeast Brazil): petrology, Sr-Nd isotopes and genetic relationships with the Paraná flood volcanics. Chemical Geology 89, 19–48.

Piccirillo, E.M., Civetta, L., Petrini, R., Longinelli, A., Bellieni, G., Comin-Chiaramonti, P., Marques, L.S., Melfi, A.J., 1989. Regional variations within the Paraná flood basalts (southern Brazil): evidence for subcontinental mantle heterogeneity and crustal contamination. Chemical Geology 75, 103–122.

Piccirillo, E.M., Melfi, A.J., 1988. The Mesozoic Flood Volcanism of the Paranà Basin: Petrogenetic and Geophysical Aspects. IAG-USP press, São Paulo, 600 pp.

Pinto, V.M., Hartmann, L.A., Santos, J.O.S., McNaughton, N.J., Wildner, W., 2011. Zircon U-Pb geochronology from the Paranà bimodal volcanic province support a brief eruptive cycle at ~135 Ma. Chemical Geology 281, 93-102.

Polo, L.A., Giordano, D., Janasi, V.A., Guimarães, L.F., 2018. Effusive silicic volcanism in the Paraná Magmatic Province, South Brazil: physico-chemical conditions of storage and eruption and considerations on the rheological behavior during emplacement. Journal of Volcanology and Geothermal Resources 355, 115–135.

Rämö, O.T., Heikkilä, P.A., Pulkkinen, A.H., 2016. Geochemistry of Paraná-Etendeka basalts from Misiones, Argentina: some new insights into the petrogenesis of high-Ti continental flood basalts. Journal of South American Earth Sciences 67, 25–39.

Raposo, M.I.B., Cañon Tapia, E., |Zhao, X., 2018. The Parana-Etendeka igneous province and related magmatism. Journal of Volcanology and Geothermal Resources, Special Issue 355.

Raposo, M.I.B., Ernesto, M., Renne, P.R., 1998. Paleomagnetism and dating of the early Cretaceous Florianópolis dyke swarm (Santa Catarina Island), Southern Brazil. Physics of the Earth and Planetary Interiors 108, 275-290.

Rapp, R.P., Watson, E.B., 1995. Dehydration melting of metabasalt at 8–32kbar: implications for continental growth and crust- mantle recycling. Journal of Petrology 36, 891–931.

Renne, P.R., Ernesto, M., Pacca, I.G., Coe, R.S., Glen, J.M., Prevot, M., Perrin, M., 1992. The age of Paraná flood volcanism, rifting of Gondwanaland, and the Jurassic-Cretaceous boundary: Science 258, 975–979.

Renne, P.R., Deckart, K., Ernesto, M., Féraud, G., Piccirillo, E.M., 1996a. Age of the Ponta Grossa dike swarm (Brazil), and implications to Paraná flood volcanism. Earth and Planetary Science Letters 144, 199–211.

Renne, P.R., Glen, J.M., Milner, S.C., Duncan, A.R., 1996b. Age of Etendeka flood volcanism and associated intrusions in southwestern Africa. Geology 24, 659–662.

Richards, M.A., Duncan, R.A., Courtillot, V.E., 1989. Flood basalts and hot-spot tracks; plume heads and tails. Science 246, 103-107.

Rivalenti, G., Mazzucchelli, M., Girardi, V.A.V., Vannucci, R., Barbieri, M.A., Zanetti, A., Goldstein, S.L., 2000. Composition and processes of the mantle lithosphere in northeastern Brazil and Fernando de Noronha: evidence from mantle xenoliths. Contributions to Mineralogy and Petrology 138, 308–325.

Rocha-Junior, E.R.V., Marques, L.S., Babinski, M., Nardy, A.J.R., Figueiredo, A.M.G., Machado, F.B., 2013. Sr-Nd-Pb isotopic constraints on the nature of the mantle sources involved in the genesis of the high-Ti tholeiites from northern Paranà Continental Flood Basalts (Brazil). Journal of South American Earth Sciences 46, 9–25.

Rosenthal, A., Yaxley, G.M., Green, D.H., Hermann, J., Kovács, I., Spandler, C., 2014. Continuous eclogite melting and variable refertilisation in upwelling heterogeneous mantle. Scientific Reports 4, 6099.

Sgualdo, P., Aviado, K., Beccaluva, L., Bianchini, G., Blichert-Toft, J., Bryce, J.G., Graham, D.W., Natali, C., Siena, F., 2015. Lithospheric mantle evolution in the Afro-Arabian domain: insights from Bir Ali mantle xenoliths (Yemen). Tectonophysics 650, 3–17.

Stanley, J.R., Flowers, R.M., Bell, D.R., 2015. Erosion patterns and mantle sources of topographic change across the southern African Plateau derived from the shallow and deep records of kimberlites. Geochemistry, Geophysics, Geosystems 16, 3235–3256.

Rossetti, L.M.M., Lima, E.F., Waichel, B.L., Hole, M.J., Simões, M.S., Scherer, C.M.S., 2018. Lithostratigraphy and volcanology of the Serra Geral Group, Paraná-Etendeka Igneous Province in Southern Brazil: towards a formal stratigraphical framework. Journal of Volcanology and Geothermal Research 355, 98–114.

Simões, M.S., Lima E.F., Rossetti L.M.M., Sommer C.A., 2019. The low-Ti high-temperature dacitic volcanism of the southern Paraná-Etendeka LIP: Geochemistry, implications for trans-Atlantic correlations and comparison with other Phanerozoic LIPs. Lithos, 342-343, 187-205.

Skjerlie, K. P. & Johnston, A. D. 1993. Fluid-absent melting behaviour of an F-rich tonalitic gneiss at mid-crustal pressures: implications for the generation of anorogenic granites. Journal of Petrology 34, 785–815.

Snoke, J.A., James, D.E., 1997. Lithospheric structure of the Chaco and Paraná Basins of South America from surface wave inversion, Journal of Geophysical Research 102, 2939–2951.

Sobolev, A.V., Hofmann, A.W., Kuzmin, D.V., Yaxley, G.M., Arndt, N.T., Chung, S.-L., Danyushevsky, L.V., Elliott, T., Frey, F.A., Garcia, M.O., Gurenko, A.A., Kamenetsky, V.S., Kerr, A.C., Krivolutskaya, N.A., Matvienkov, V.V., Nikogosian, I.K., Rocholl, A., Sigurdsson, I.A., Sushchevskaya, N.M., Teklay, M., 2007. The amount of recycled crust in sources of mantle-derived melts. Science 316, 412–417.

Sobolev, A.V., Sobolev, S.V., Kuzmin, D.V., Malitch, K.N., Petrunin, A.G., 2009. Siberian meimechites: origin and relation to flood basalts and kimberlites. Russian Geology and Geophysics 50, 999–1033.

Stewart, K., Turner, S., Kelley, S., Hawkesworth, C., Kirstein, L., Mantovani, M., 1996. 3-D, ^{40}Ar-^{39}Ar geochronology in the Paraná continental flood basalt province. Earth and Planetary Science Letters 143, 95–109.

Stewart, K., Kelley, S., Turner, S., Hawkesworth, C., Mantovani, M., 1994. 3-D 40Ar-39Ar geochronology in the Paraná flood basalt province. Mineralogical Magazine 58A, 879-880.

Stracke, A., 2012. Earth's heterogeneous mantle: a product of convection-driven interac- tion between crust and mantle. Chemical Geology 330-331, 274–299.

Stroncik, N.A., Trumbull, R.B., Krienitz, M-S., Niedermann, S., Romer, R.L., Harris, C., Day, J.M.D., 2017. Helium isotope evidence for a deep-seated mantle plume involved in South Atlantic breakup. Geology 45, 827-830.

Sun, S.S., McDonough, W.F., 1989. Chemical and isotopic systematics of oceanic basalts: implications for mantle composition and processes. Geological Society of London (GSL) Special Publications 42, 313–347.

Tan, E., Gurnis, M., Han, L.J., 2002. Slabs in the lower mantle and their modulation of plume formation. Geochemistry Geophysics Geosystems 3, 1067.

Thiede, D.S., Vasconcelos, P.M., 2010. Paraná flood basalts: rapid extrusion hypothesis confirmed by new $^{40}Ar/^{39}Ar$ results. Geology 38, 747–750.

Thordarson, T., Larsen, G., 2007. Volcanism in Iceland in historical time: Volcano types, eruption styles and eruptive history. Journal of Geodynamics 43, 118–152.

Thompson, R.N., Gibson, S.A., Dickin, A.P., Smith, P.M., 2001. Early Cretaceous basalt and picrite dikes of the southern Etendeka region, NW Namibia: Windows into the role of the Tristan mantle plume in Paraná–Etendeka magmatism. Journal of Petrology 42, 2049–2081.

Thy, P., Beard, J. S. & Lofgren, J. E. 1990. Experimental constraints on the origin of Icelandic rhyolites. Journal of Geology 98, 417–21.

Tuff, J., Takahashi, E., Gibson, S.A., 2005. Experimental constraints on the role of garnet pyroxenite in the in the genesis of high-Fe mantle plume derived melts. Journal of Petrology 46, 2223–2258.

Turner, S., Regelous, M., Kelly, S., Hawkesworth, C., Mantovani, M., 1994. Magmatism and continental break-up in the South Atlantic: $^{40}Ar/^{39}Ar$ geochronology. Earth and Planetary Science Letters 121, 333–348.

Turner, S., Hawkesworth, C.J., Gallagher, K., Stewart, K., Peate, D.W., Mantovani, M.S.M., 1996. Mantle plumes, flood basalts and thermal models for melt generation beneath continents: assessment of a conductive heating model and application to the Paraná. Journal of Geophysical Research 101, 11503–11518.

van der Lee, S., James, D., Silver, P., 2001. Upper mantle S velocity structure of central and western South America. Journal of Geophysical Research 106, 30821 – 30834.

Vidotti, R.M., Ebinger, C.J., Fairhead, J.D., 1998. Gravity signature of the western Paraná Basin, Brazil. Earth and Planetary Science Letters, 159, 117–132,

White, R.W., McKenzie, D.P., 1989. Magmatism at rift zones: the generation of volcanic continental margins and flood basalts. Journal of Geophysical Research 94, 7685–7729.

Walter, M.J., 1998. Melting of garnet peridotite and the origin of komatiite and depleted lithosphere. Journal of Petrology 39, 29–60.

Weaver, B.L., 1991. The Origin of Ocean Island Basalt End-Member Compositions: Trace Element and Isotopic Constraints. Earth and Planetary Science Letters 104, 381-397.

White, W.M., 2010. Oceanic Island Basalts and Mantle Plumes: The Geochemical Perspective. Annual Review of Earth and Planetary Sciences. Annual Review of Earth and Planetary Sciences, 38, 133-160.

Whittingham, A.M., 1991. Stratigraphy and petrogenesis of the volcanic formations associated with the opening of the South Atlantic, southern Brazil. Ph.D. Thesis, Univ. Oxford, 162 pp.

Wolf, M.B., Wyllie, P.J., 1994. Dehydration-melting of amphibolite at 10 kbar: The effects of temperature and time. Contribution to Mineralogy and Petrology 115, 369-383.

Zalan, P.V., Wolff, S., Conceicao, C.J., Astolfi, M.A.M., Vieira, I.S., Appi, V.T., Zanotto, O.A., Marques, A., 1987. Tectonics and sedimentation of the Paranà Basin. Proceedings of the VII International Gondwana Symposium, São Paulo, Brazil, p. 83-117.

Zhang, Y., Liu, J., Guo, Z., 2010. Permian basaltic rocks in the Tarim basin, NW China: implications for plume-lithosphere interaction. Gondwana Research 18, 596–610.

Figure captions

Figure 1 – Paleogeographic reconstruction of Paranà-Etendeka CFB at 135–130 Ma (modified after Natali et al., 2018, and Buchan and Ernst 2019, for circurmferential dykes). HT and LT spatial distribution was reviewed after data from Piccirillo and Melfi (1988), Piccirillo et al. (1989 and 1990), Hawkesworth et al. (1992); Garland et al.(1995); Peate et al. (1999), Marzoli et al. (1999); Marsh et al. (2001); Thompson et al. (2001),;Ewart et al. (2004 a and b) Lustrino et al. (2005), Cernuschi et al. (2015), Marsh and Swart (2016), Rämö et al. (2016); Licht (2018); HT and LT suites from Etendeka and Angola include the respective silicic differentiates. Locations of early alkaline complexes (145–138 Ma) after Gibson et al. (2006), Comin-Chiaramonti et al.(2007 and 2014); Gomes and Comin - Chiaramonti Eds.(2017).

Figure 2 (a) Total Alkali-Silica (TAS) classification diagram (after Le Bas, 1986) for HT (picrite basalt to trachydacites) and LT (picrite basalt to dacite-rhyolites) suites from Paranà-Etendeka Province. (b) TiO_2 *vs* MgO variation diagram for basaltic rocks. An empirical boundary between HT (Paranapanema, Pitanga, Urubici in Paranà; Khumib and Doros in Etendeka) and LT (Esmeralda, Gramado in Paranà; Horingbai and Tafelberg in Etendeka) is drawn in order to minimize the misclassified samples (generally less than 5 %). Data from GEOROC database (http://georoc.mpch-mainz.gwdg.de/georoc/).

Figure 3 MgO *vs* FeO diagram for Paranà-Etendeka CFB. HT and LT primary magmas were modelled according to Herzberg and Asimow (2015); liquid lines of descent by fractional crystallisation and removal of olivine (Ol) plagioclase (Pl) and clinopyroxene Cpx) according to Danyushevsky and Plechov (2011). Data are from GEOROC database.

Figure 4 Chondrite (Ch)-normalized Rare Earth Element (REE) patterns for HT and LT Paranà - Etendeka basaltic rocks modified after Natali et al. (2018). Average La_N/Yb_N for each group is also reported. Normalising factors are from Sun and McDonough (1989). Data are from GEOROC database.

Figure 5 Primitive mantle (PM)-normalized incompatible element distribution of calculated HT and LT primary melts for Etendeka (a) and Paranà (b). The batch melting modelled compositions, using source mode and melting proportions according to Walter (1998) and partition coefficients (*Kd*) from GERM data base, give the following indications: 1) PM source slightly hybridized by 3% eclogite is appropriate for generating the Etendeka HT and LT primary magmas by ~ 9 to 22% partial melting (F), respectively (*cfr.* Natali et al., 2018); 2) PM source, could produce Paranà HT and LT primary magmas by ~ 10% to 24% F, respectively; provided that an appropriate enrichment of LREE and LFSE (from 1.5 to 5 x PM) would be considered in the source; 3) the ubiquitous residual garnet predicted by the model is in accordance with thermobarometric estimates and conforms to deep melting events (P > 3 GPa). Normalising factors are from Sun and McDonough (1989). See text for further explanation.

.

Figure 6 (a) Sr-Nd and (b) Pb isotopic compositions of CFB for Paranà-Etendeka basaltic rocks, modified after Natali et al. (2018). To be noted the remarkable isotopic diversity between the least contaminated CFB from Paranà and Etendeka (data from GEOROC). Isotopic composition of Gough and Tristan hot spot tracks are from Hoernle et al. (2015). Compositional field of regional continental basement is after Garland et al. (1995), whereas crustal contamination trend is taken from Hoernle et al. (2015). Reference mantle end-members (DM, EMI, EMII, HIMU and FOZO) are also reported for comparison (Stracke, 2012).

Figure 7 Computed liquid lines of descent (LLD) starting from inferred parental basalts are reported for HT (blue) and LT (red) of Paranà-Etendeka suites. Modelling has been performed by PELE (Boudreau, 1999) assuming redox QFM+1 /QFM H_2O 0.4–0.3wt% and P 0.05 GPa.

Figure 8 Cumulative diagram of crystallising minerals (wt.%) predicted by PELE model (Boudreau, 1999) for HT and LT inferred parental basalts of Paranà-Etendeka. In both suites olivine crystallisation is followed by plagioclase and clinopyroxene at T ~ 1170 and 1140–1100 C°, respectively. Precipitation of Fe-Ti oxides, soon followed by apatite, occurs at T 1070–1040 C°. Late crystallization orthopyroxene appears only in LT suites. Abbreviations: Ol = olivine, Cpx = clinopyroxene, Pl = plagioclase, Opx = orthopyroxene, Hm-Ilm = hematite–ilmenite, Mt-Usp = magnetite–ulvospinel, Ap = apatite

Figure 9 (a, b) Primordial Mantle (PM)-normalised incompatible elements and **(c, d)** Chondrite (Ch)-normalised Rare Earth Elements (REE) distribution for LT and HT parental basalts and silicic differentiates from Paranà-Etendeka. The fractionation modelling has been performed by PELE software (Boudreau, 1999), integrating the partition coefficient database with data from Mahood and Stimac (1990). Model results satisfactorily fit the composition of HT trachydacites and LT dacite-rhyolites as 13–15% residual liquids from the assumed parental basalts. Normalisation factors are from Sun and McDonough (1989).

Figure 10 V and Cr *vs* Zr variation diagrams for LT **(a, c)** and HT **(b, d)** basaltic to silicic rocks from Paranà-Etendeka. Fractional crystallisation (FC) by PELE software and batch melting (BM) models have been tested for generation of silicic differentiates in the two suites starting from the respective basalt compositions; figures indicate melting proportion for BM.
Note that only fractional crystallisation satisfactorily fits the differentiation trends to trachydacites and dacite-rhyolites in HT and LT suites, respectively. Partition coefficients (*Kd*) from GERM database. Rock symbols as in Fig. 2

Figure 11 **(a)** Sr-Nd and **(b)** Pb isotopic compositions of basaltic and silicic rocks for the Paranà-Etendeka province. Compositional field of regional continental basement is after Garland et al (1995), whereas crustal contamination trend is taken from Hoernle et al. (2015). Data from GEOROC. Rock symbols as in Fig. 2

Figure 12 **(a)** Interpretative cross-section (not to scale) between of the Paranà plateau and Etendeka region demonstrating the intensive extension and block faulting during the rifting stage. Both the HT and LT magmas partly experienced differentiation during rising in the continental crust: 1) continuous intracrustal FC of HT magmas (in blue) that led to the trachy-dacite differentiates that erupted mostly as limited lavas and dykes; 2) due to their higher viscosity, the LT magmas (in red) tended to be trapped in shallow crustal chambers undergoing AFC processes to dacite-rhyolites before erupting as rheo-ignimbrites; **(b)** the calculated viscosity for HT and LT suites are calibrated for anhydrous (PELE model) and variably hydrated conditions at 950 °C and 900 °C, respectively (Giordano et al., 2008; Polo et al., 2018). For the Paranà acidic differentiates of both suites, the combined effect of temperatures (T 1000–900 °C) and water contents (H_2O 1–2. wt %; Garland et, al, 1995, Lucchetti et al., 2018; PELE model) resulted in viscosity values lower that those commonly recorded for explosive eruptions of silicic magmas. However, the higher viscosity and discharge rates characterising LT dacite-rhyolites allowed these magmas to attain the hydrodynamic/brittle fragmentation limit (shaded area: Namikia and Manga, 2008; Gonnermann and Manga, 2012), producing extensive high-grade (low explosivity) rheo-ignimbrites.

Figure 13 – **(a)** Approximated areal distribution of CFB magmatism related to Paranà plateau *s.s.* and rifting stages. The circles denote the inferred focus of the tectonomagmatic activity migrating south-eastward from the first impact of the proto-Tristan plume in (1) central Paranà to the (2) Etendeka margin. **(b)** The protracted impinging of the mantle plume head on the Gondwana plate resulted in a remarkable thermal anomaly (T_{ex} 250–300 °C) that generated the Paranà Plateau CFBs (135–134 Ma) from the lower lithosphere at P= 3–4 GPa and T_p=1500–1550 °C. **(c)** The continuous thermal-mechanical effects of the rising plume, concomitant with the northwest Gondwana drift, resulted in the progressive arching, thinning, and rifting of the lithosphere that culminated in the South American/African continental breakup close to the Etendeka border. This stage is characterised by the bimodal distribution of the basalts to silicic products in both the HT and LT suites and the exclusive appearance of high-MgO basalts/picrites which represent the deepest and hottest (P of up to 5 GPa and T_p of up to 1590 °C) sub-lithospheric melts from the plume axial zone. The thermal regime and composition of the sub-continental lithosphere is based on mantle xenoliths from the Gondwana realm: Sp- to Gt-lherzolite/harzburgite (Rivalenti et al., 2000; Fodor et al., 2002; Dessai et al., 2004; Griffin et al., 2003; Beccaluva et al., 2007; 2008; 2011; Karmalkar et al., 2009; Natali et al., 2013; Bianchini et al., 2014; Sgualdo et al., 2015; Stanley et al., 2016).

Declaration of interests

The authors declare that they have no known competing financial interests or personal relationships that could have appeared to influence the work reported in this paper.

Sincerely,
Luigi Beccaluva and co-Authors

Highlights

- Paranà-Etendeka LIP developed in two stages, triggered by a plume impingement
- In the first stage, Paranà plateau *s.s.* CFB derived from lithospheric sources
- In the second stage, Etendeka CFB formed from plume-related sources during rifting

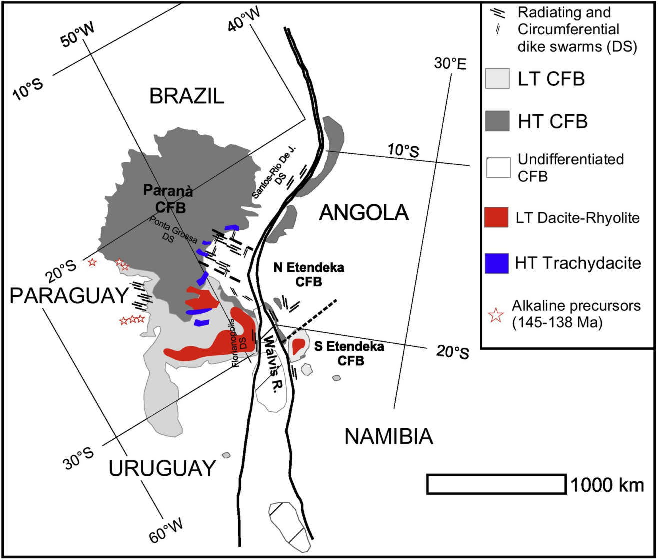
Radiating and Circumferential dike swarms (DS)
LT CFB
HT CFB
Undifferentiated CFB
LT Dacite-Rhyolite
HT Trachydacite
Alkaline precursors (145-138 Ma)
50°W
40°W
10°S
30°E
BRAZIL
10°S
Paranà CFB
Santos-Rio De J. DS
Ponta Grossa DS
ANGOLA
20°S
PARAGUAY
N Etendeka CFB
Florianopolis DS
Walvis R.
S Etendeka CFB
20°S
NAMIBIA
30°S
URUGUAY
1000 km
60°W

Figure 1

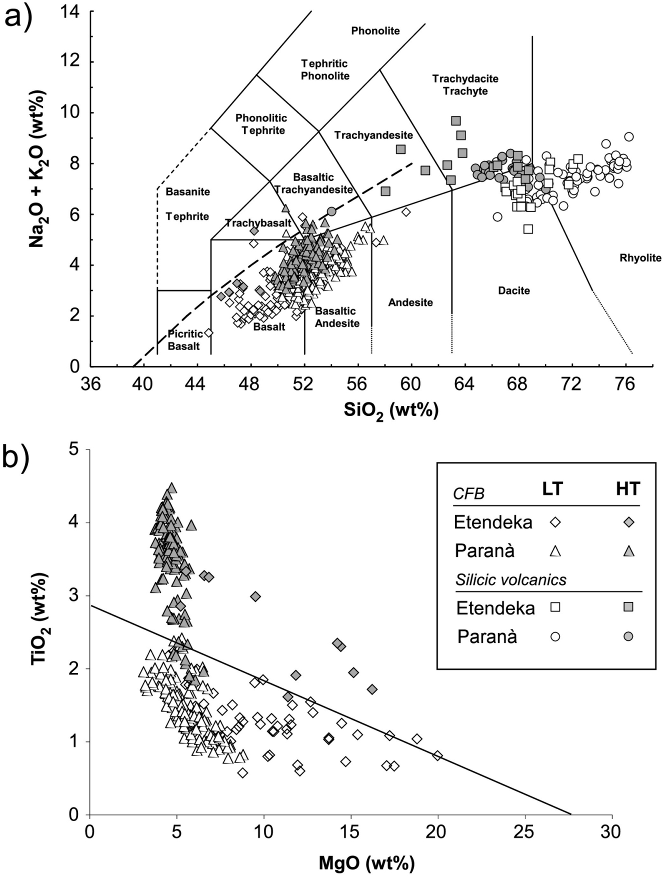
a)
Na2O + K2O (wt%)
SiO2 (wt%)
Phonolite
Tephritic Phonolite
Trachydacite Trachyte
Phonolitic Tephrite
Trachyandesite
Basaltic Trachyandesite
Basanite
Tephrite
Trachybasalt
Rhyolite
Dacite
Andesite
Basaltic Andesite
Basalt
Picritic Basalt
b)
TiO2 (wt%)
MgO (wt%)
CFB
LT
HT
Etendeka
Paranà
Silicic volcanics
Etendeka
Paranà

Figure 2

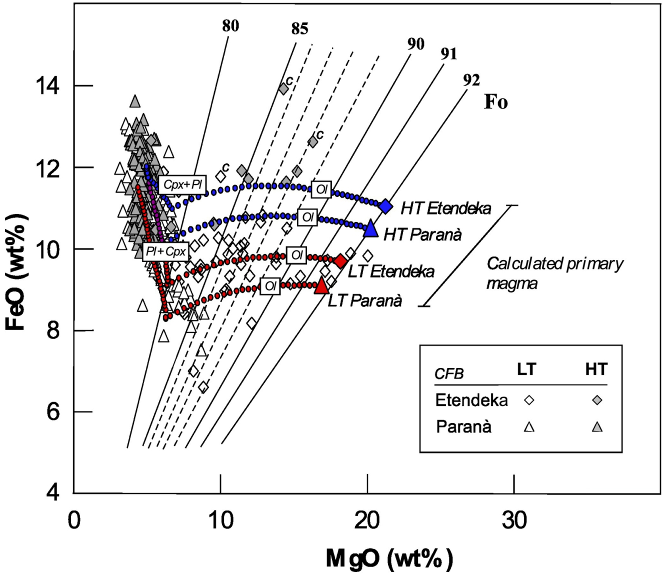

80
85
90
91
92
Fo
14
12
10
8
6
4
FeO (wt%)
0
10
20
30
MgO (wt%)
c
c
c
Cpx+Pl
Pl+Cpx
Ol
Ol
Ol
Ol
HT Etendeka
HT Paranà
LT Etendeka
LT Paranà
Calculated primary magma
CFB
LT
HT
Etendeka
Paranà

Figure 3

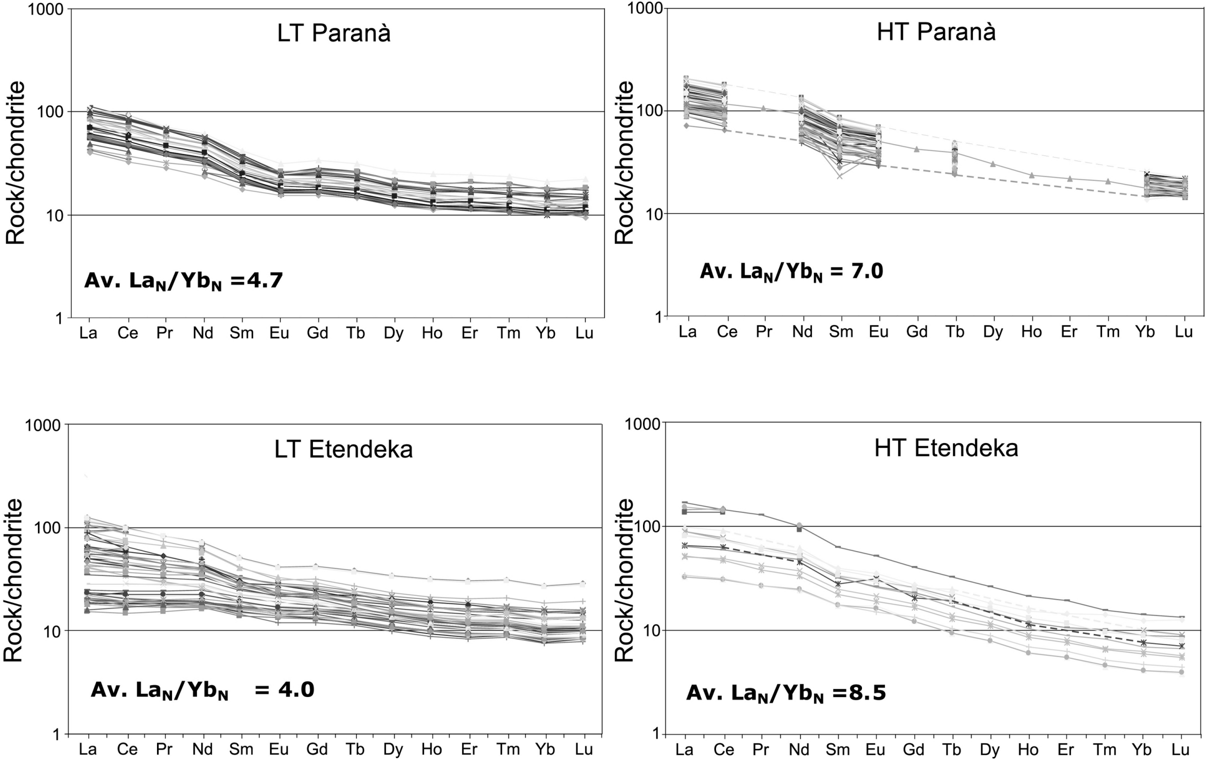
LT Paranà
Rock/chondrite
1000
100
10
1
La Ce Pr Nd Sm Eu Gd Tb Dy Ho Er Tm Yb Lu
Av. La_N/Yb_N =4.7
HT Paranà
Av. La_N/Yb_N = 7.0
LT Etendeka
Av. La_N/Yb_N = 4.0
HT Etendeka
Av. La_N/Yb_N =8.5

Figure 4

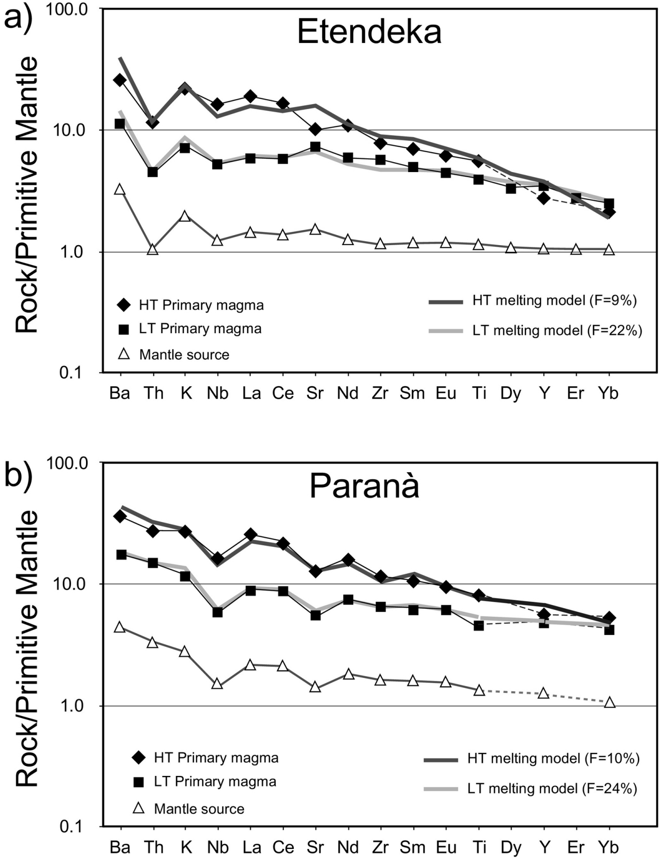
a)
Etendeka
Rock/Primitive Mantle
100.0
10.0
1.0
0.1
HT Primary magma
LT Primary magma
Mantle source
HT melting model (F=9%)
LT melting model (F=22%)
Ba Th K Nb La Ce Sr Nd Zr Sm Eu Ti Dy Y Er Yb
b)
Paranà
Rock/Primitive Mantle
100.0
10.0
1.0
0.1
HT Primary magma
LT Primary magma
Mantle source
HT melting model (F=10%)
LT melting model (F=24%)
Ba Th K Nb La Ce Sr Nd Zr Sm Eu Ti Dy Y Er Yb

Figure 5

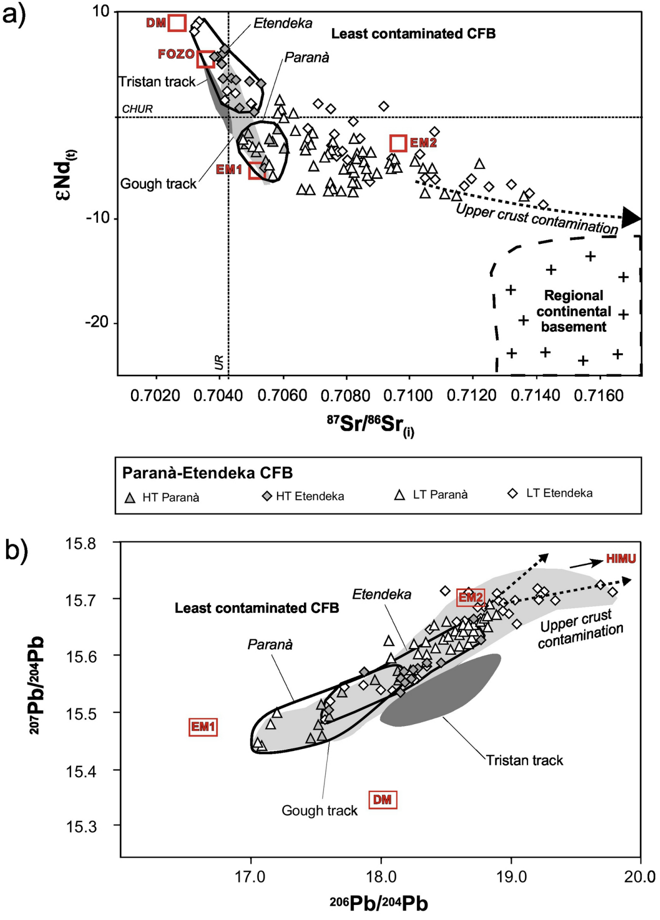

a)
10
-10
-20
DM
FOZO
EM1
EM2
Etendeka
Paranà
Least contaminated CFB
Tristan track
CHUR
Gough track
Upper crust contamination
Regional continental basement
UR
εNd(t)
0.7020
0.7040
0.7060
0.7080
0.7100
0.7120
0.7140
0.7160
87Sr/86Sr(i)
Paranà-Etendeka CFB
HT Paranà
HT Etendeka
LT Paranà
LT Etendeka
b)
15.8
15.7
15.6
15.5
15.4
15.3
207Pb/204Pb
Least contaminated CFB
Etendeka
Paranà
EM1
EM2
HIMU
DM
Upper crust contamination
Tristan track
Gough track
17.0
18.0
19.0
20.0
206Pb/204Pb

Figure 6

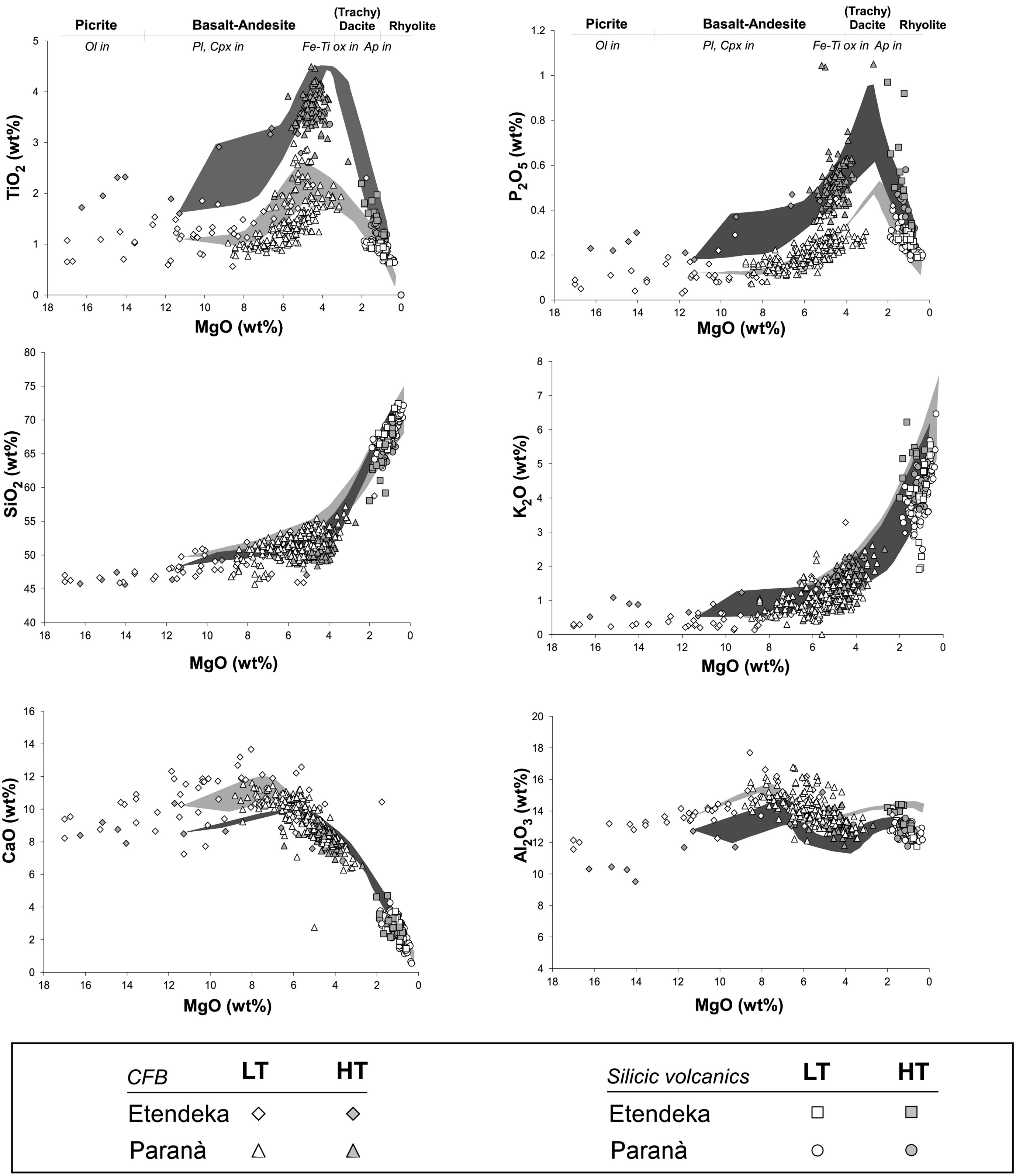
Picrite
Basalt-Andesite
(Trachy) Dacite
Rhyolite
Ol in
Pl, Cpx in
Fe-Ti ox in
Ap in
TiO2 (wt%)
P2O5 (wt%)
SiO2 (wt%)
K2O (wt%)
CaO (wt%)
Al2O3 (wt%)
MgO (wt%)
CFB
LT
HT
Etendeka
Paranà
Silicic volcanics
LT
HT
Etendeka
Paranà

Figure 7

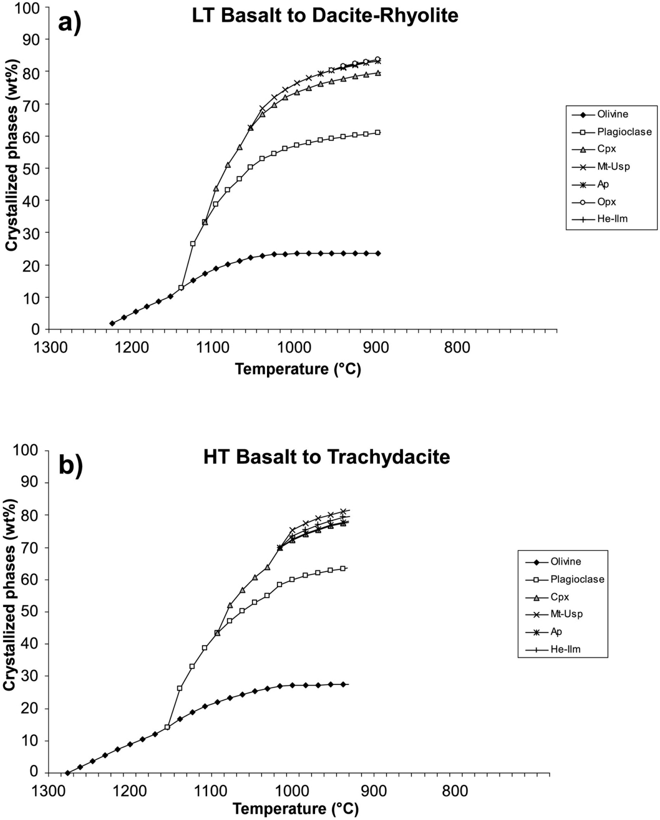
a)
LT Basalt to Dacite-Rhyolite
Crystallized phases (wt%)
Temperature (°C)
Olivine
Plagioclase
Cpx
Mt-Usp
Ap
Opx
He-Ilm
b)
HT Basalt to Trachydacite
Crystallized phases (wt%)
Temperature (°C)
Olivine
Plagioclase
Cpx
Mt-Usp
Ap
He-Ilm

Figure 8

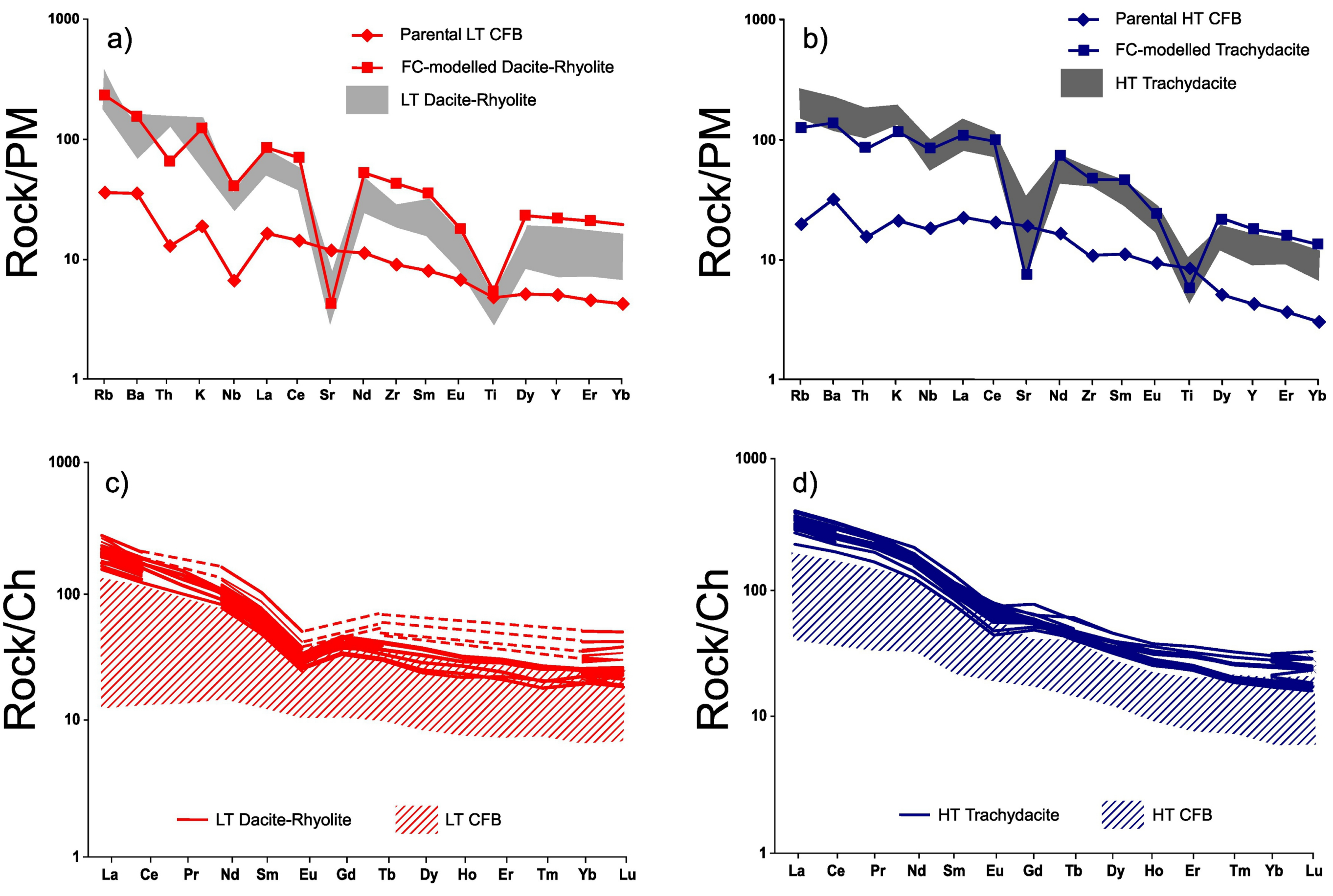
a)
Parental LT CFB
FC-modelled Dacite-Rhyolite
LT Dacite-Rhyolite
Rock/PM
1000
100
10
1
Rb Ba Th K Nb La Ce Sr Nd Zr Sm Eu Ti Dy Y Er Yb
b)
Parental HT CFB
FC-modelled Trachydacite
HT Trachydacite
Rock/PM
1000
100
10
1
Rb Ba Th K Nb La Ce Sr Nd Zr Sm Eu Ti Dy Y Er Yb
c)
Rock/Ch
1000
100
10
1
LT Dacite-Rhyolite
LT CFB
La Ce Pr Nd Sm Eu Gd Tb Dy Ho Er Tm Yb Lu
d)
Rock/Ch
1000
100
10
1
HT Trachydacite
HT CFB
La Ce Pr Nd Sm Eu Gd Tb Dy Ho Er Tm Yb Lu

Figure 9

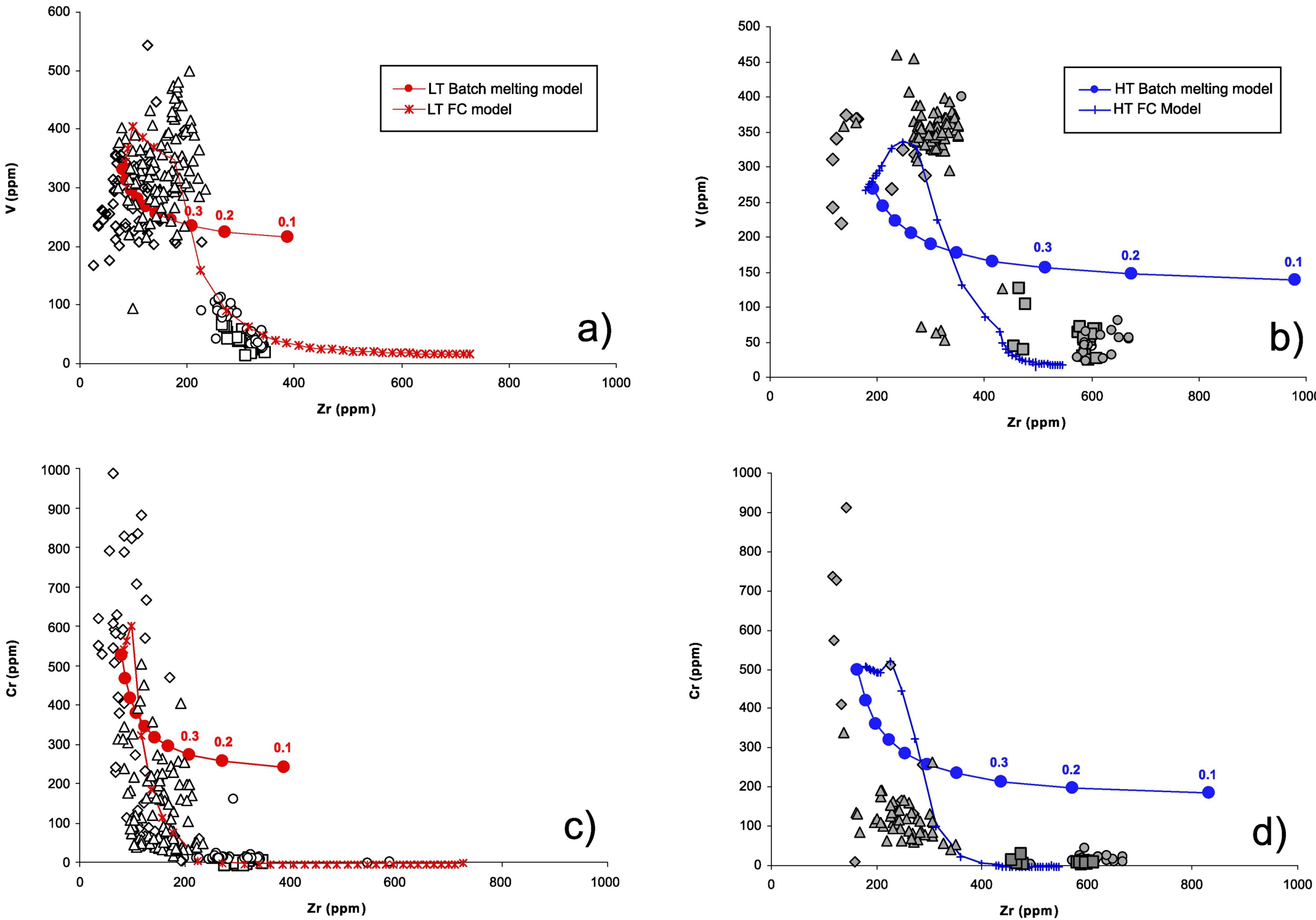

a)
V (ppm)
Zr (ppm)
LT Batch melting model
LT FC model
0.3
0.2
0.1
b)
HT Batch melting model
HT FC Model
c)
Cr (ppm)
d)

Figure 10

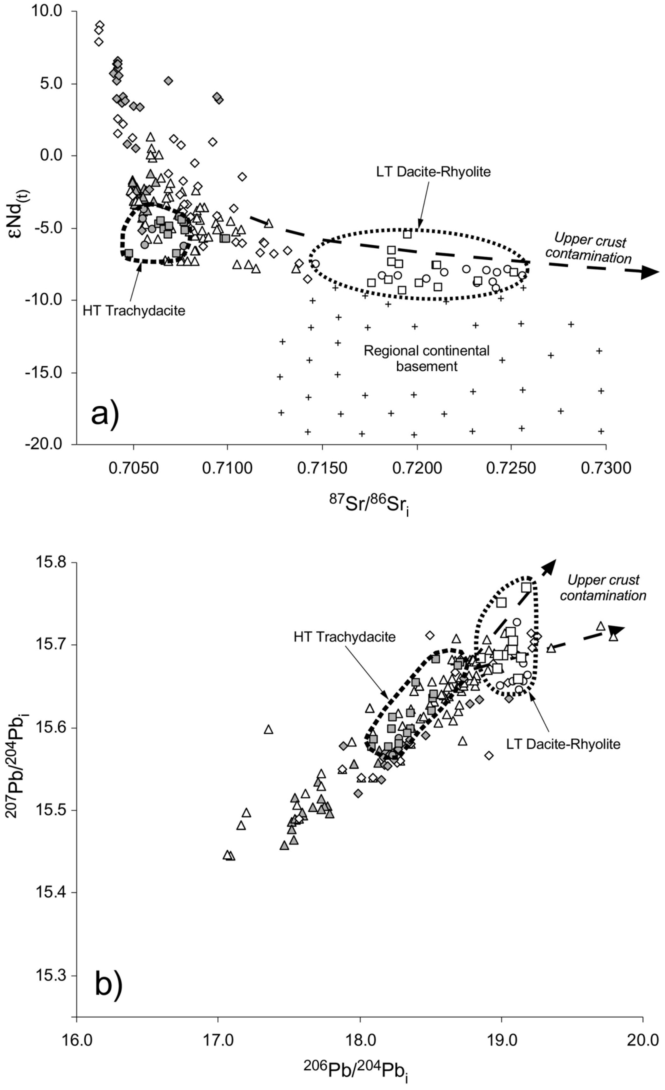

10.0
5.0
0.0
-5.0
-10.0
-15.0
-20.0
εNd(t)
0.7050
0.7100
0.7150
0.7200
0.7250
0.7300
87Sr/86Sri
LT Dacite-Rhyolite
Upper crust contamination
HT Trachydacite
Regional continental basement
a)
15.8
15.7
15.6
15.5
15.4
15.3
207Pb/204Pbi
16.0
17.0
18.0
19.0
20.0
206Pb/204Pbi
Upper crust contamination
HT Trachydacite
LT Dacite-Rhyolite
b)

Figure 11

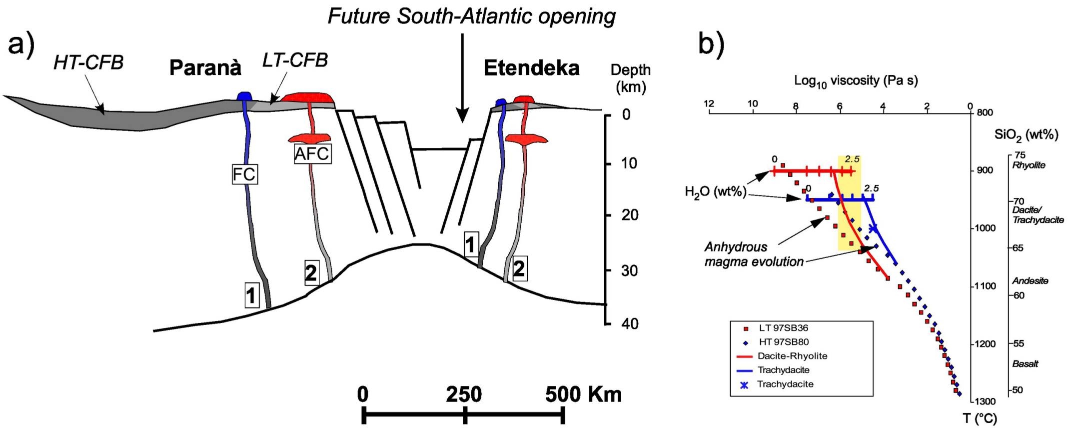

a)
Future South-Atlantic opening
HT-CFB
Paranà
LT-CFB
Etendeka
Depth (km)
0
10
20
30
40
FC
AFC
1
2
1
2
0
250
500 Km
b)
Log10 viscosity (Pa s)
12
10
8
6
4
2
0
800
900
1000
1100
1200
1300
T (°C)
SiO2 (wt%)
75
Rhyolite
70
Dacite/ Trachydacite
65
Andesite
60
55
Basalt
50
H2O (wt%)
0
2.5
0
2.5
Anhydrous magma evolution
LT 97SB36
HT 97SB80
Dacite-Rhyolite
Trachydacite
Trachydacite

Figure 12

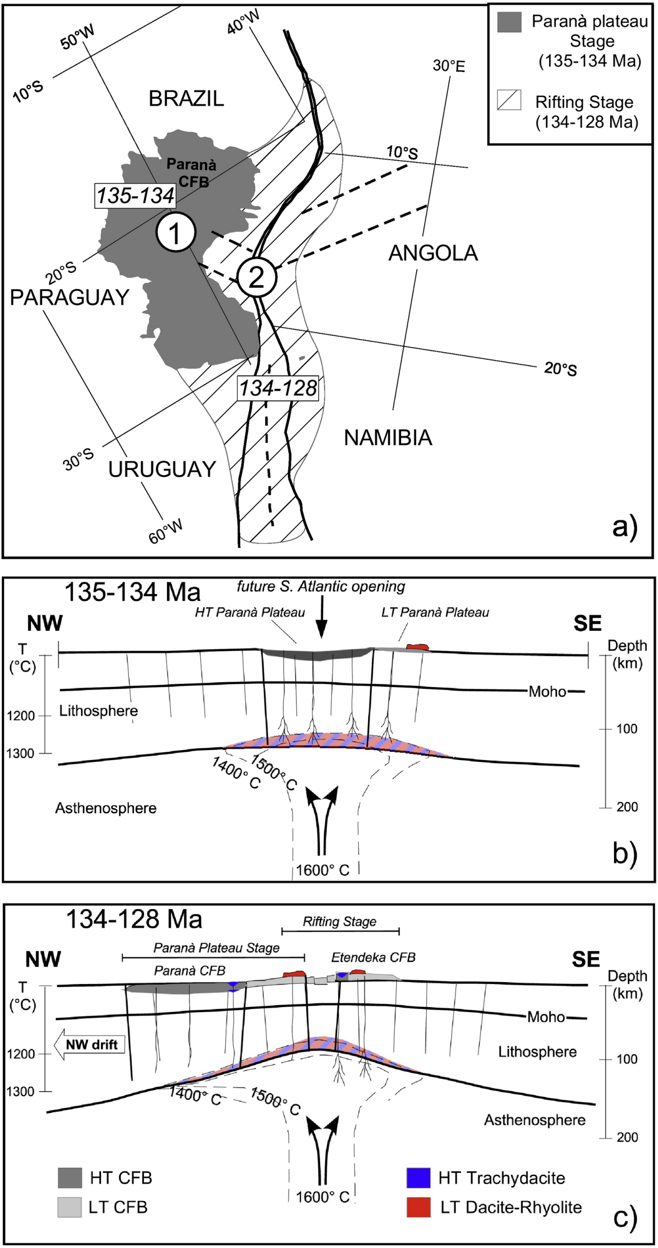
Paranà plateau Stage (135-134 Ma)
Rifting Stage (134-128 Ma)
10°S
50°W
40°W
30°E
BRAZIL
Paranà CFB
135-134
1
2
10°S
ANGOLA
20°S
PARAGUAY
20°S
134-128
NAMIBIA
30°S
URUGUAY
60°W
a)
135-134 Ma
future S. Atlantic opening
HT Paranà Plateau
LT Paranà Plateau
NW
SE
T (°C)
Depth (km)
Moho
Lithosphere
1200
1300
100
1400° C
1500° C
Asthenosphere
200
1600° C
b)
134-128 Ma
Rifting Stage
Paranà Plateau Stage
Etendeka CFB
Paranà CFB
NW
SE
T (°C)
Depth (km)
Moho
NW drift
Lithosphere
1200
100
1300
1400° C
1500° C
Asthenosphere
200
HT CFB
LT CFB
1600° C
HT Trachydacite
LT Dacite-Rhyolite
c)

Figure 13